Supporting Information

Inverse Design of Nanoclusters for Light-Controlled CO_2–HCOOH Interconversion

Wei Pei, Pengju Wang, Si Zhou*, Jijun Zhao

Key Laboratory of Materials Modification by Laser, Ion and Electron Beams (Dalian University of Technology), Ministry of Education, Dalian 116024, China

*Corresponding author, e-mail: sizhou@dlut.edu.cn

S1. Computational methods

The inverse design based on genetic algorithm program (IDOGA), inherits from our early version of CGA code,[1] which contains the essential procedure for global minimization of the potential energy surface (PES) of clusters within the framework of genetic algorithm. During the IDOGA search, IDOGA is based on a population of individuals, each individual representing a cluster structure. The evolutionary principles are adopted to identify the optimal cluster structure. 8 ~ 20 members of initial population are generated for a fixed cluster formula, and the global search lasts for 2000 ~ 4000 iterations. All the isomer structures produced by the standard "crossover + mutation" operation are optimized by density functional theory (DFT) calculations implemented in the DMol^3 program,[2] using the double numerical basis including *d* and *p* polarization function (DNP), and the Perdew, Burke, and Ernzerhof (PBE) functional within the generalized gradient approximation (GGA).[3] The HOMO-LUMO gaps from PBE calculations are corrected by the Heyd-Scuseria-Ernzerhof (HSE06) hybrid functional to ensure the efficiency of IDOGA search and meanwhile guarantee the accuracy of estimated gaps (see Figure S1).[4] The rotational inertia and eigenvalue of adjacent matrix are calculated to ensure no isomorphic structures in populations. At the final iteration, the 10 members of cluster isomers with smallest F are considered as the candidate catalysts for each formula.

S2. Testing data of different software and functionals

Table S1. HOMO-LUMO gap (in unit of eV) of selective Pd_xS_y clusters calculated by different methods including the VASP code using PAW potentials combined with the PBE functional or HSE06 hybrid functional, respectively, and the Gaussian 09 program using the aug-cc-pvdz all electron basis set combined with the PBE functional or HSE06 hybrid functional, respectively.

	VASP		Gaussian	
	PBE	HSE06	PBE	HSE06
Pd_2S_3	0.91	2.06	0.80	2.07
Pd_2S_4	1.06	1.92	0.96	1.86
Pd_3S_5	0.96	1.91	0.79	1.90
Pd_4S_5	0.83	1.87	0.76	1.88
Pd_4S_6	1.02	1.79	0.80	1.76
Pd_4S_7	1.23	2.17	1.13	2.17
Pd_5S_5	0.83	1.83	0.77	1.86
Pd_5S_6	0.90	1.78	0.77	1.78
Pd_5S_7	1.18	1.97	1.07	2.24
Pd_5S_9	0.95	1.85	0.97	1.97
Pd_6S_6	0.91	1.79	0.77	1.77

Table S2. Adsorption energy of CO_2 molecule (in unit of eV) on selective Pd_xS_y clusters calculated by different methods including the VASP code using Grimme's D3 correction, PAW potentials, combined with the PBE functional or HSE06 hybrid functional, respectively, and the Gaussian 09 program using the aug-cc-pvdz all electron basis set combined with the PBE functional or HSE06 hybrid functional, respectively.

	VASP		Gaussian	
	PBE	HSE06	PBE	HSE06
Pd_2S_3	−0.98	−0.70	−0.91	−0.70
Pd_2S_4	−0.82	−0.61	−0.76	−0.63
Pd_3S_5	−0.46	−0.61	−0.51	−0.45
Pd_4S_5	−0.45	−0.39	−0.30	−0.43
Pd_4S_6	−0.46	−0.44	−0.47	−0.42
Pd_4S_7	−0.57	−0.54	−0.50	−0.56
Pd_5S_5	−0.46	−0.42	−0.45	−0.43
Pd_5S_6	−0.70	−0.62	−0.68	−0.65
Pd_5S_7	−0.51	−0.47	−0.54	−0.45
Pd_5S_9	−0.58	−0.49	−0.52	−0.47
Pd_6S_6	−0.47	−0.46	−0.49	−0.45

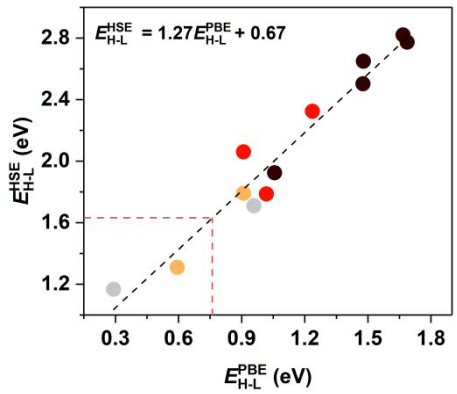

Figure S1. Comparison between the HOMO-LUMO gap of Pd_xS_y clusters calculated by the HSE06 hybrid functional ($E_{\text{H-L}}^{\text{HSE}}$) and PBE functional ($E_{\text{H-L}}^{\text{PBE}}$). According to our systematic test, the HOMO-LUMO gaps predicted by these two functionals have a scaling relation with each other as $E_{\text{H-L}}^{\text{HSE}} = 1.27\ E_{\text{H-L}}^{\text{PBE}} + 0.67$. To speed up the IDOGA search, the PBE functional is used for geometric optimization during the iterations of global search, with the HOMO-LUMO gaps of Pd_xS_y clusters corrected by the HSE06 hybrid functional based on the scaling relation to ensure the accuracy of estimated gaps in the objective function.

S3. Structures of Pd_xS_y clusters

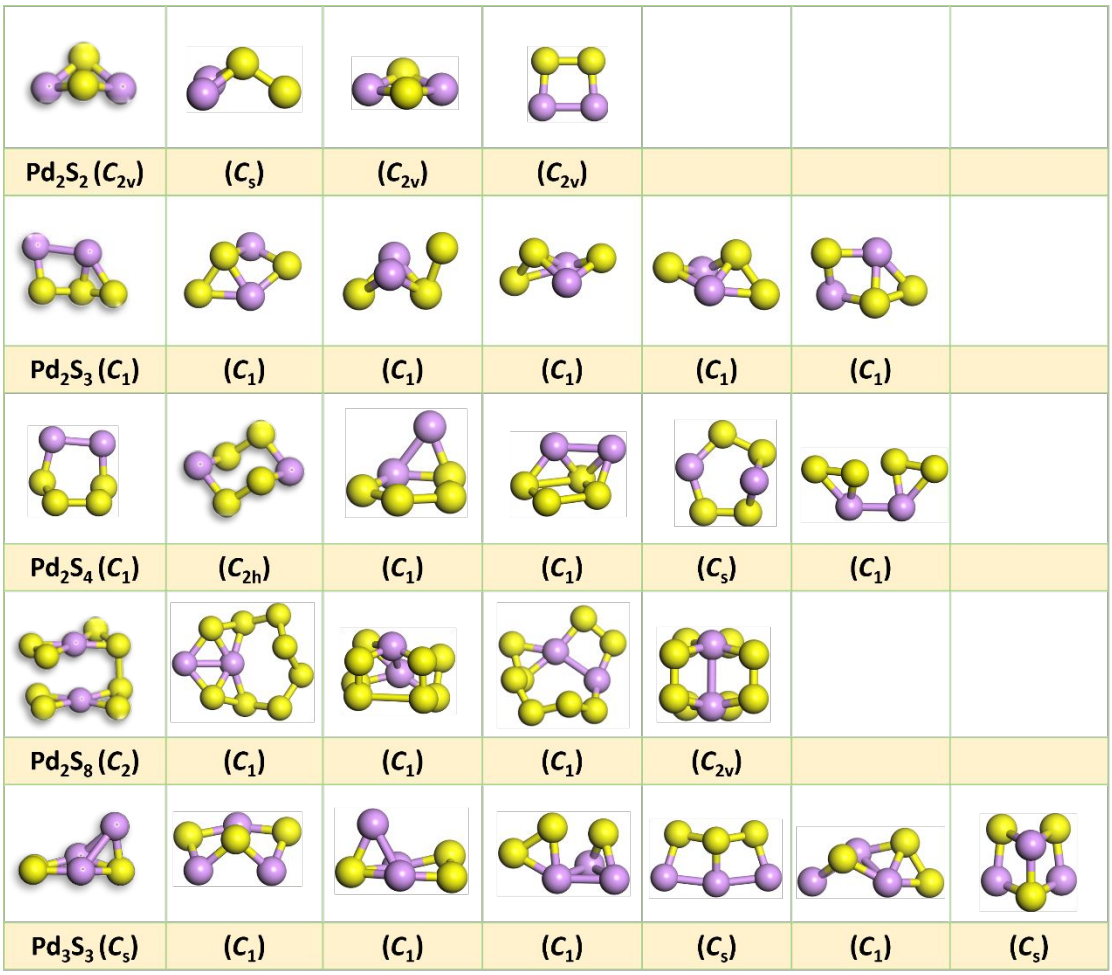

Figure S2. Structures of the ground-state (the first left panel in each row) and low-lying isomers of Pd_xS_y clusters with different stoichiometries. The Pd and S atoms are shown in purple and yellow colors, respectively.

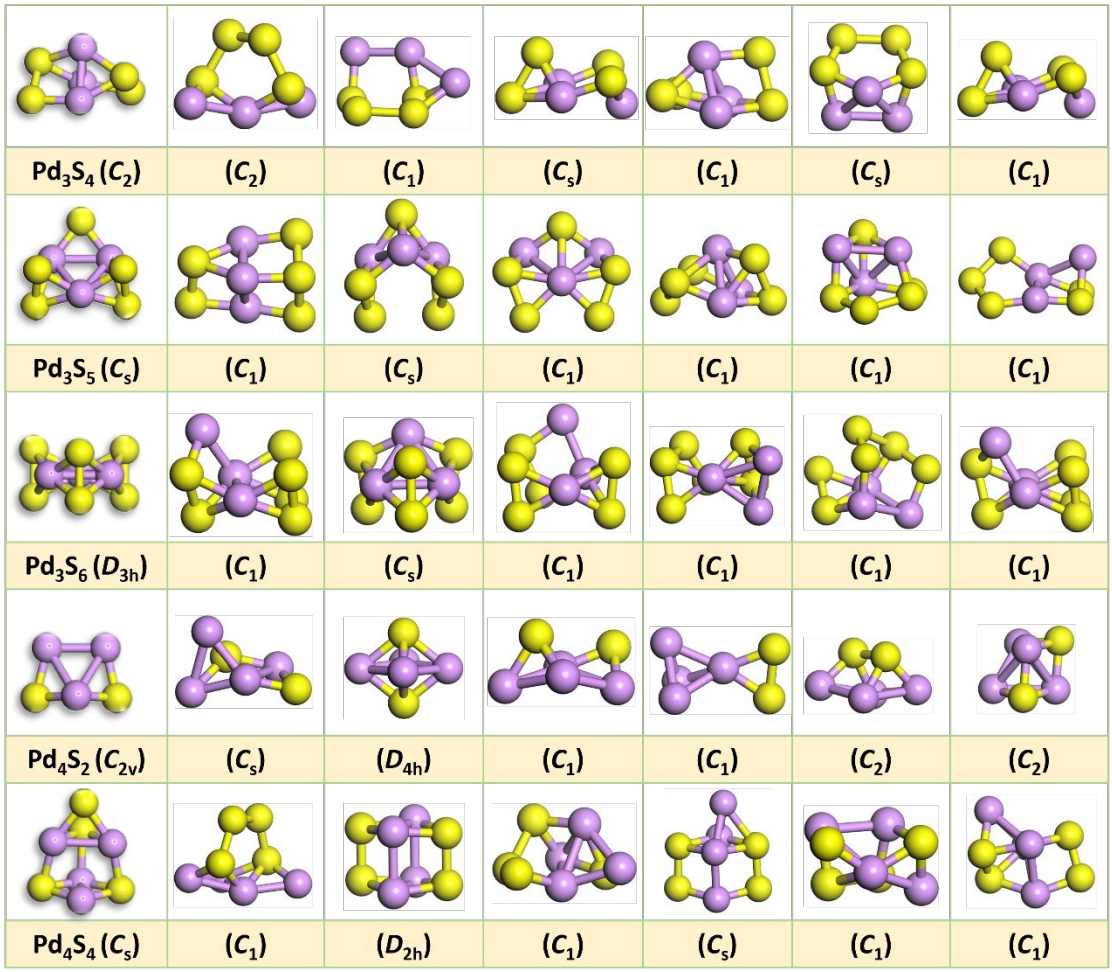

Figure S3. Structures of the ground-state (the first left panel in each row) and low-lying isomers of Pd_xS_y clusters with different stoichiometries. The Pd and S atoms are shown in purple and yellow colors, respectively.

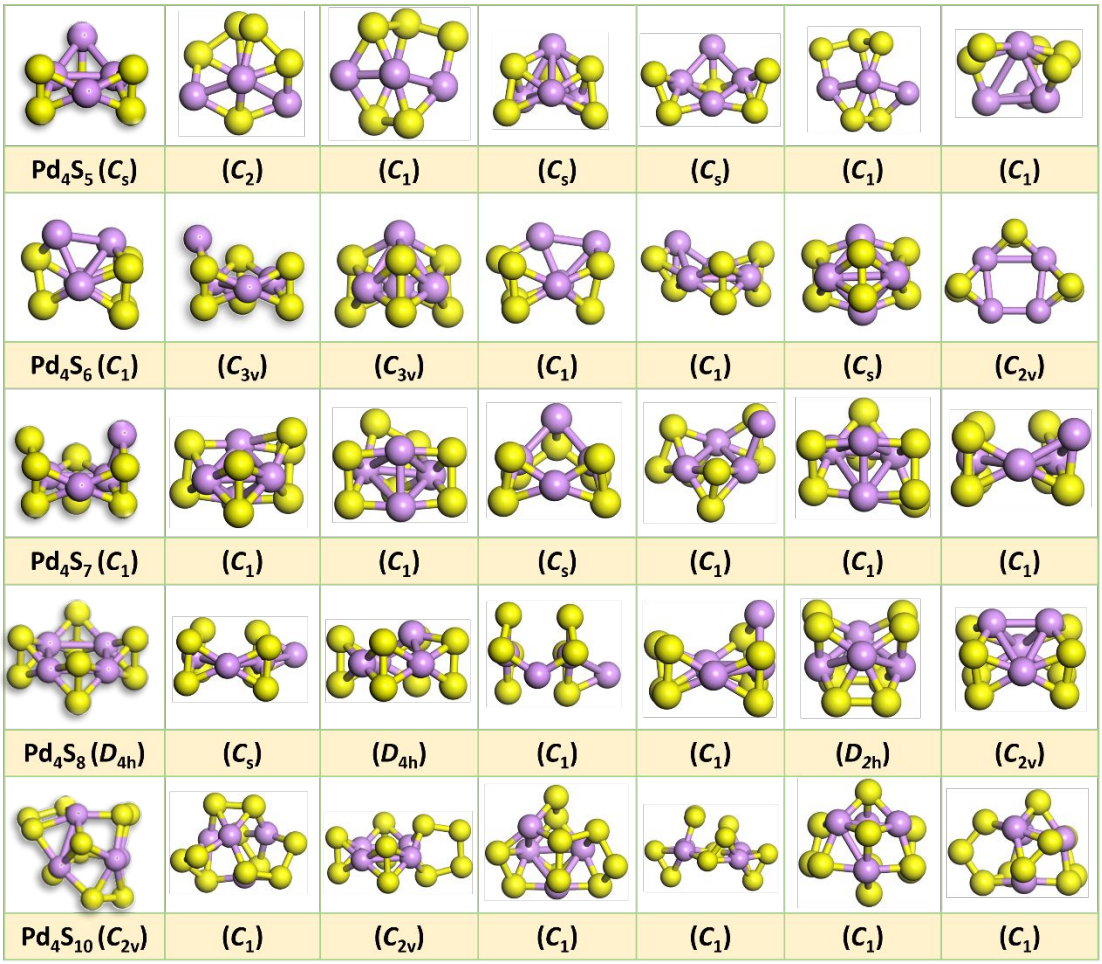

Figure S4. Structures of the ground-state (the first left panel in each row) and low-lying isomers of Pd_xS_y clusters with different stoichiometries. The Pd and S atoms are shown in purple and yellow colors, respectively.

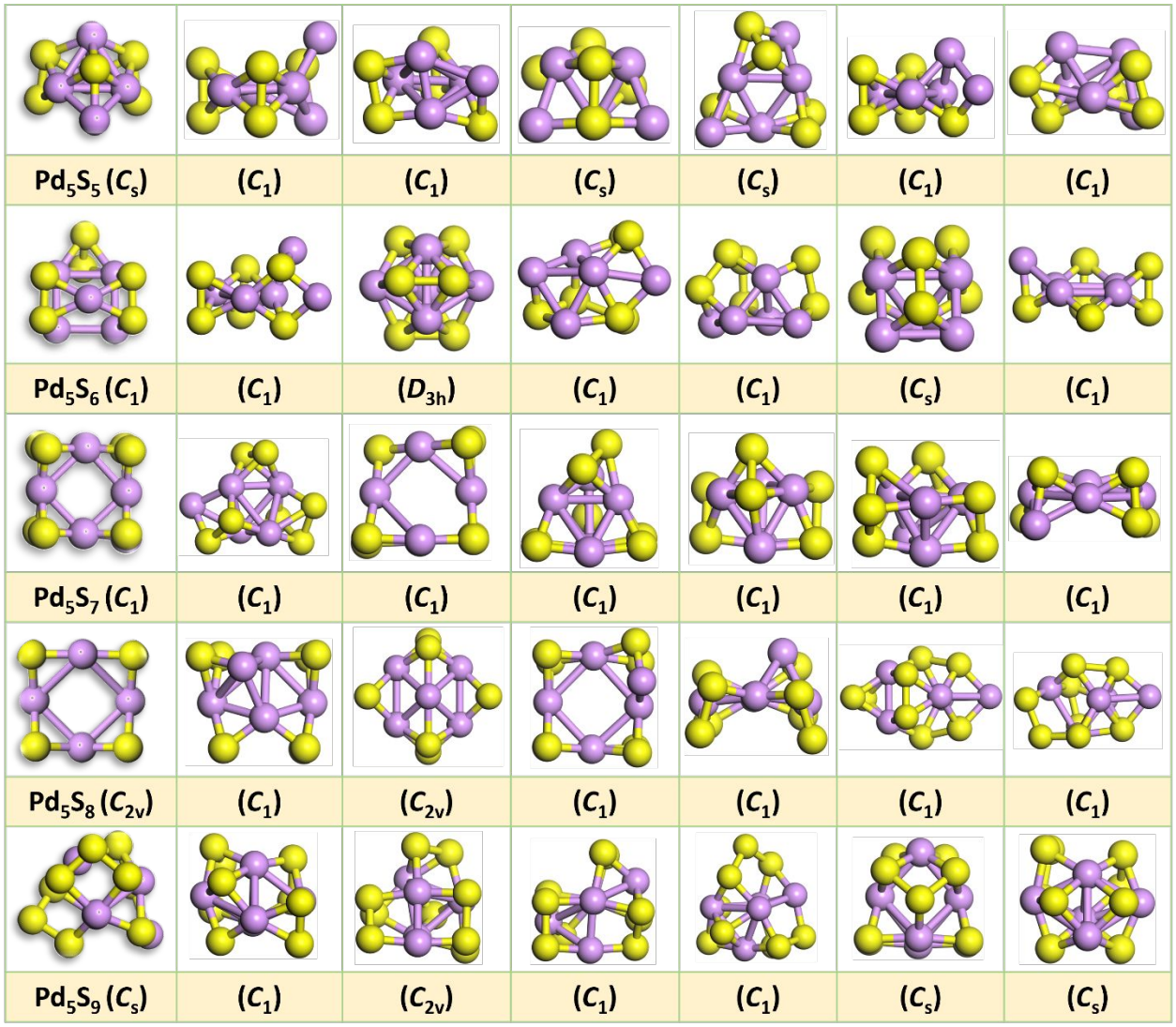

Figure S5. Structures of the ground-state (the first left panel in each row) and low-lying isomers of Pd_xS_y clusters with different stoichiometries. The Pd and S atoms are shown in purple and yellow colors, respectively.

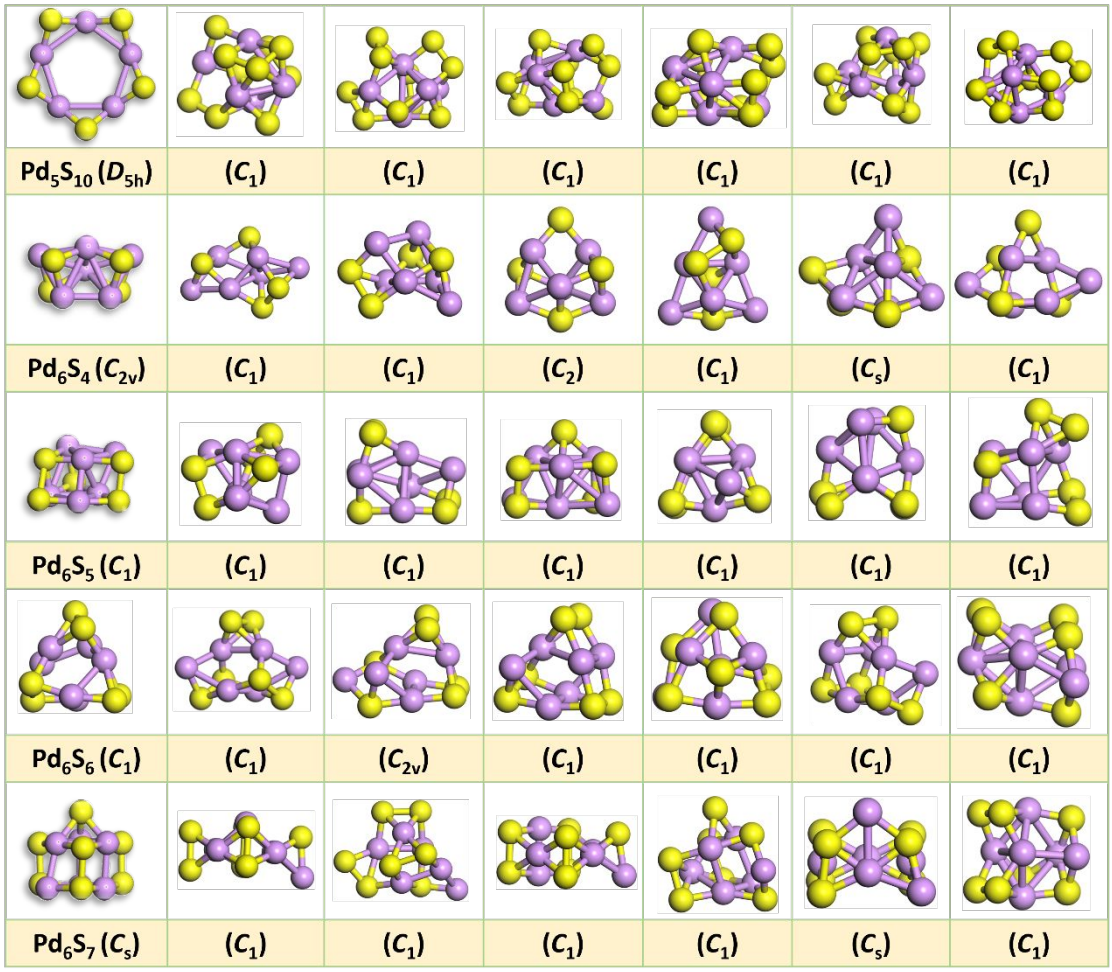

Figure S6. Structures of the ground-state (the first left panel in each row) and low-lying isomers of Pd_xS_y clusters with different stoichiometries. The Pd and S atoms are shown in purple and yellow colors, respectively.

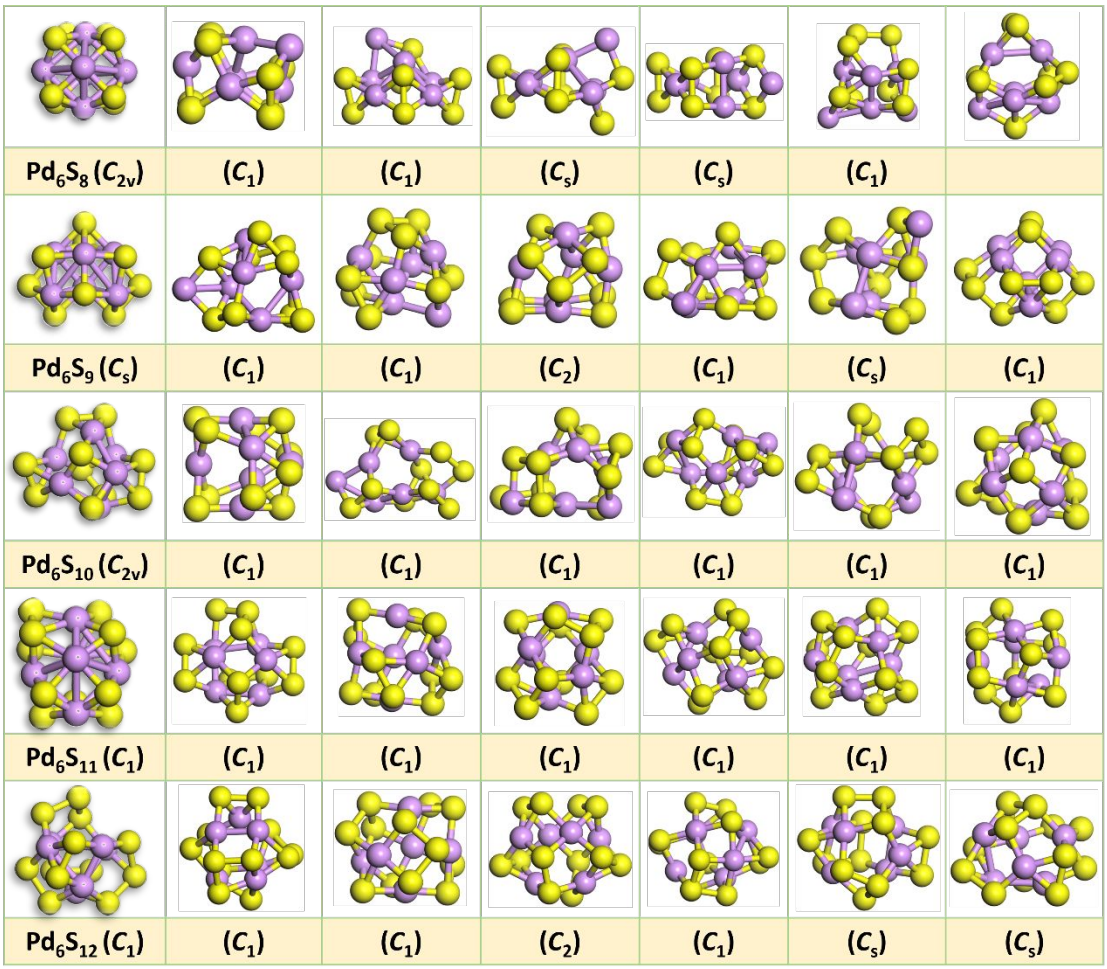

Figure S7. Structures of the ground-state (the first left panel in each row) and low-lying isomers of Pd_xS_y clusters with different stoichiometries. The Pd and S atoms are shown in purple and yellow colors, respectively.

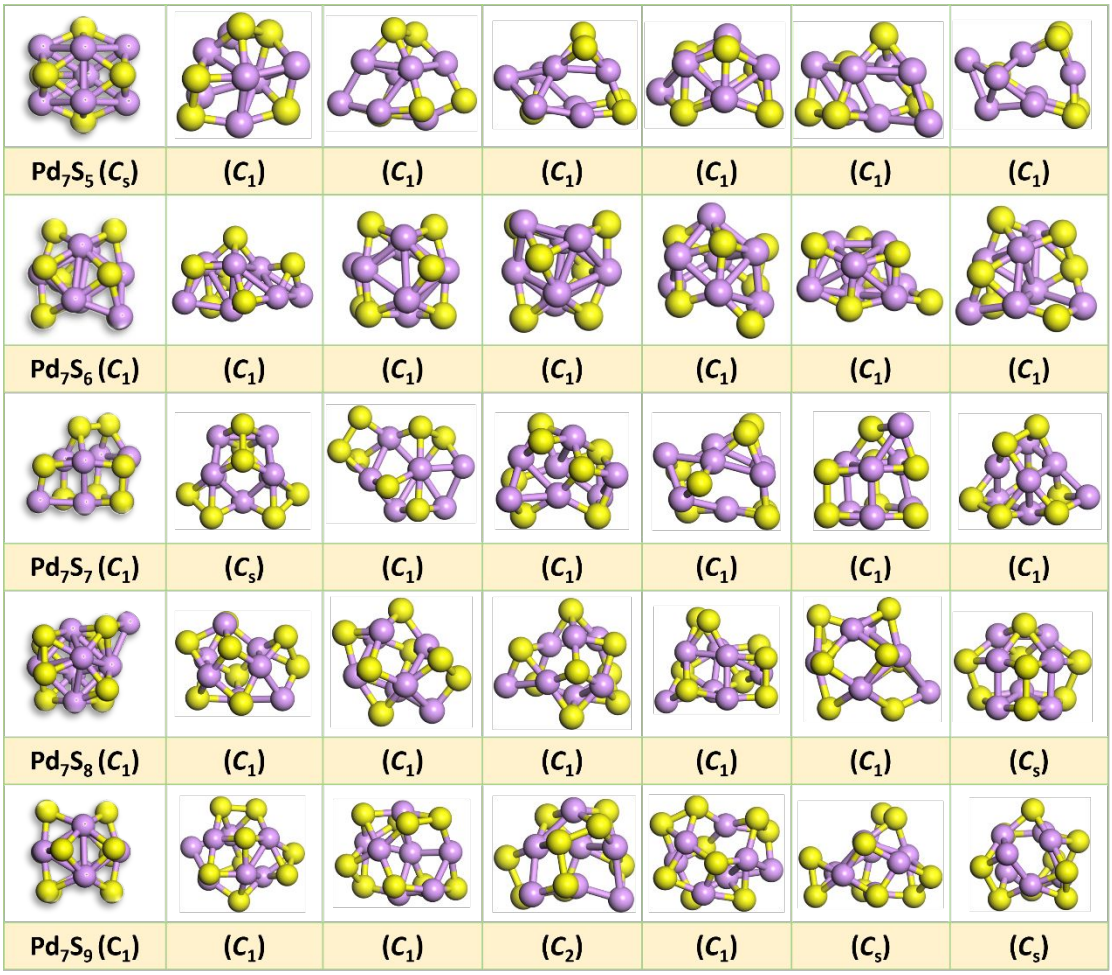

Figure S8. Structures of the ground-state (the first left panel in each row) and low-lying isomers of Pd_xS_y clusters with different stoichiometries. The Pd and S atoms are shown in purple and yellow colors, respectively.

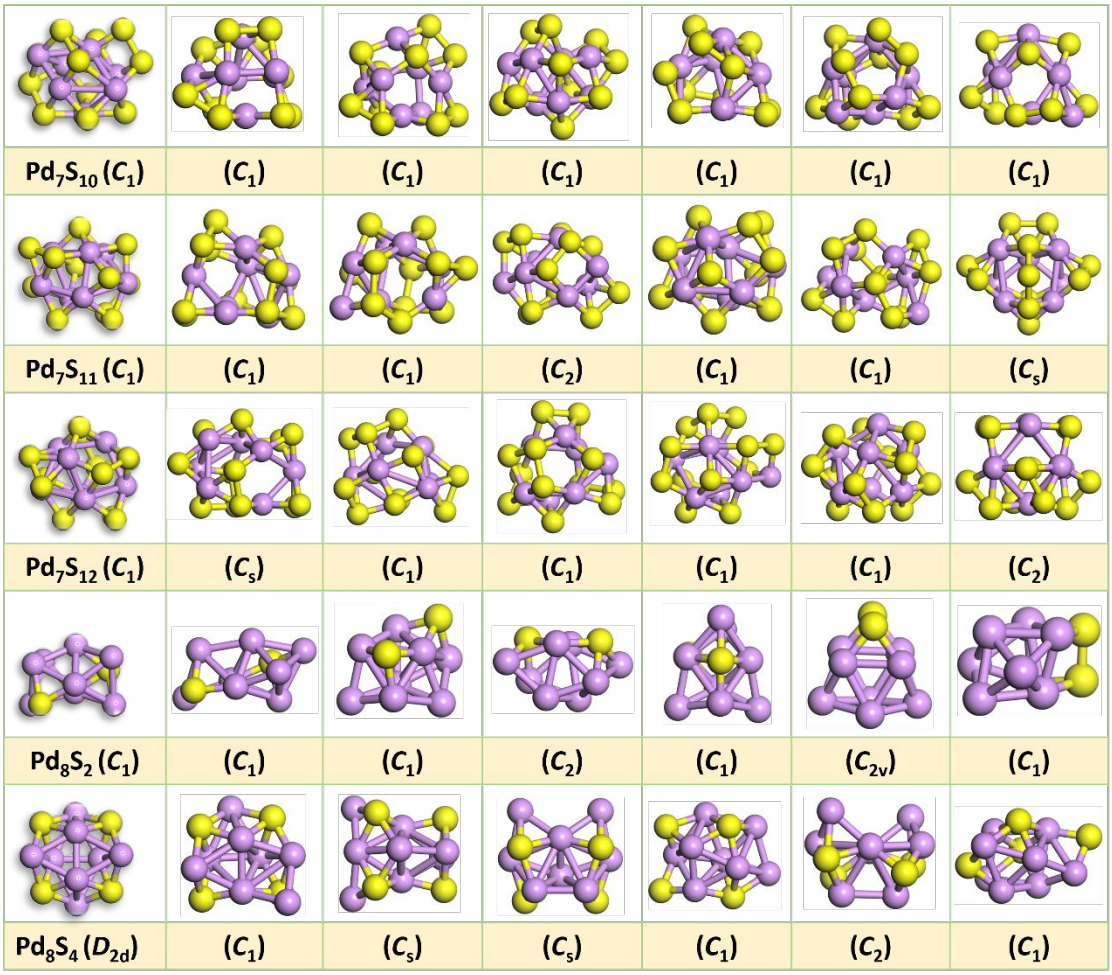

Figure S9. Structures of the ground-state (the first left panel in each row) and low-lying isomers of Pd_xS_y clusters with different stoichiometries. The Pd and S atoms are shown in purple and yellow colors, respectively.

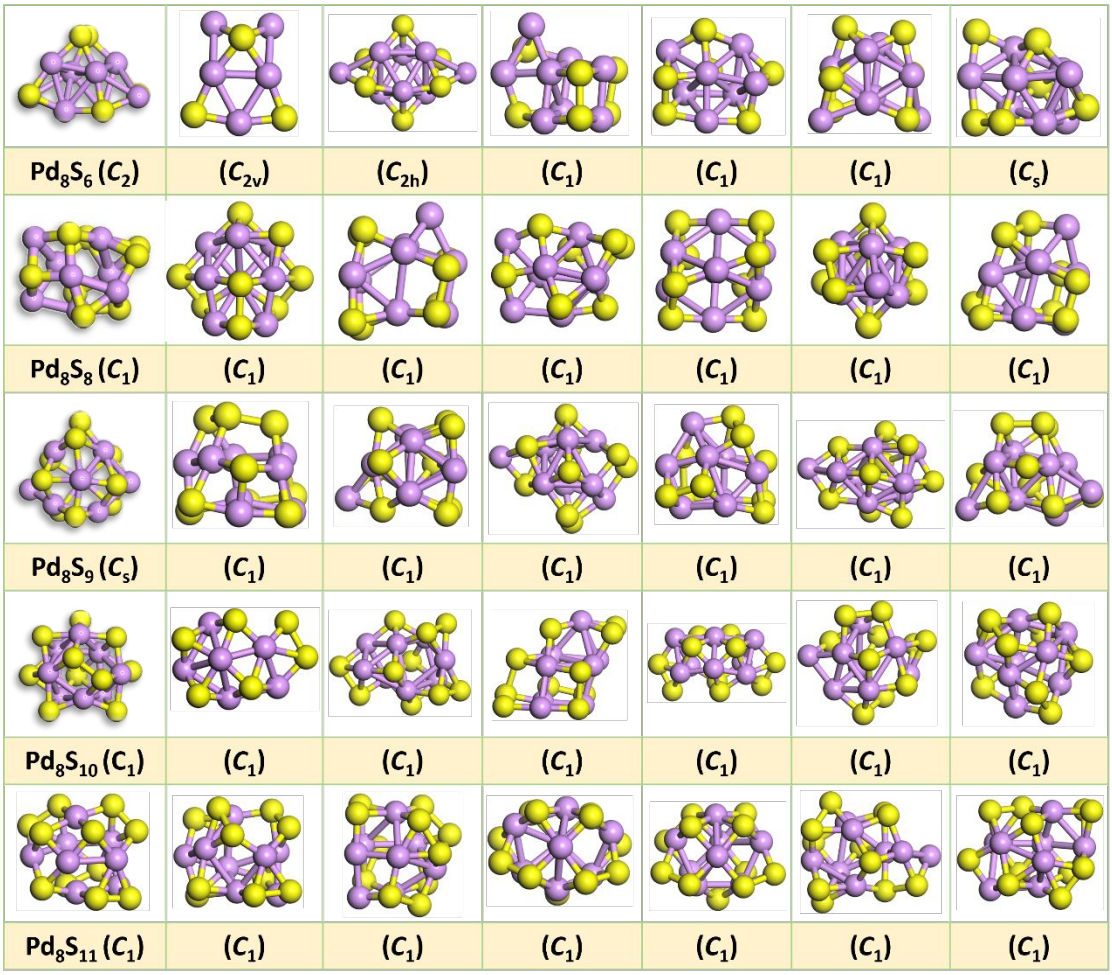

Figure S10. Structures of the ground-state (the first left panel in each row) and low-lying isomers of Pd_xS_y clusters with different stoichiometries. The Pd and S atoms are shown in purple and yellow colors, respectively.

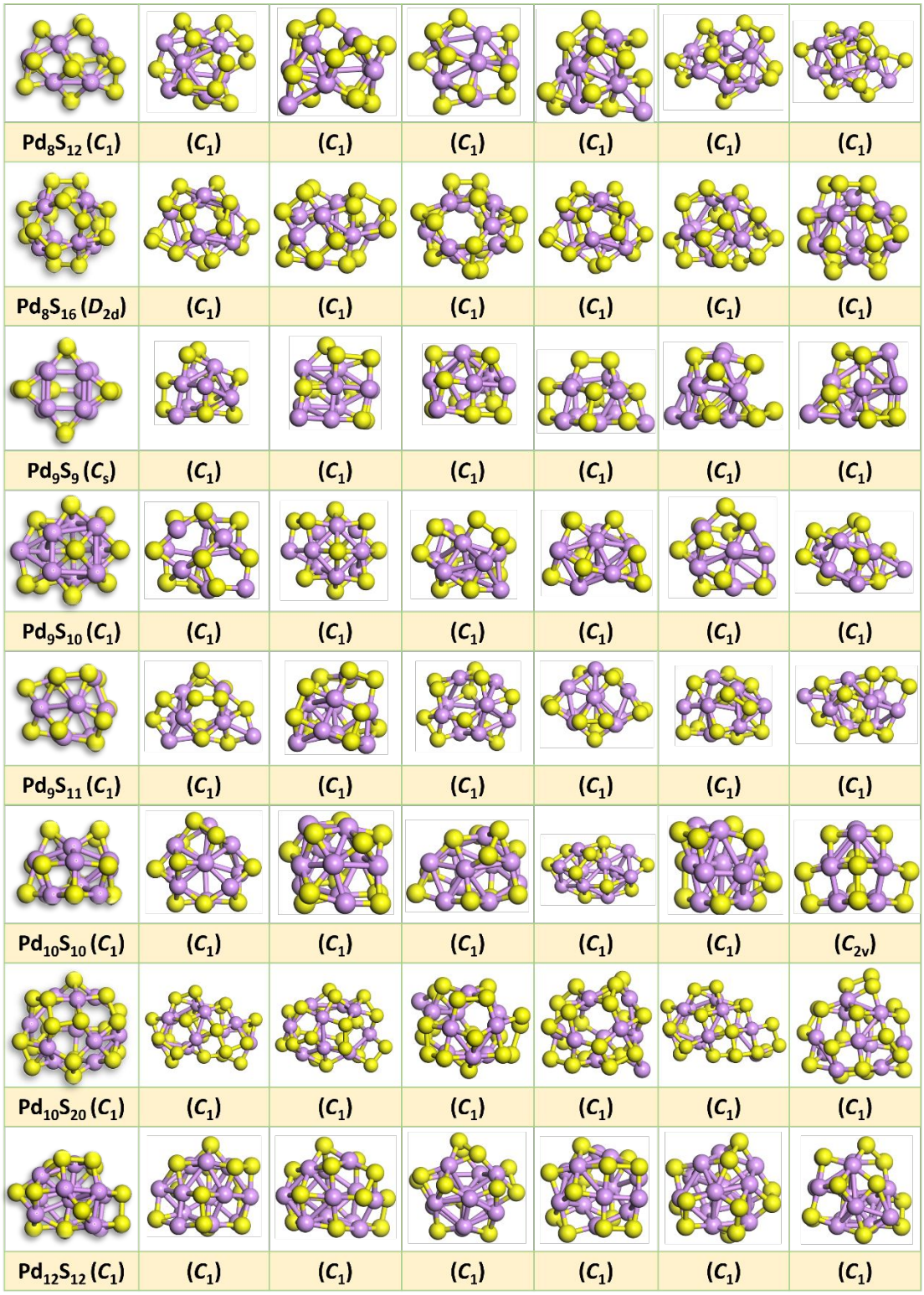

Figure S11. Structures of the ground-state (the first left panel in each row) and low-lying isomers of Pd_xS_y clusters with different stoichiometries. The Pd and S atoms are shown in purple and yellow colors, respectively.

Table S3. The key parameters of optimized Pd_xS_y clustes, inlcuding HOMO-LUMO gap ($E_{\text{H-L}}^{\text{HSE}}$), LUMO levels (LUMO), reduction power (U_e), adsorption energies of chemisorbed CO_2 molecule. The Pd_xS_y clusters in the ground states are marked in black, and those metastable isomers are marked in blue.

System	Isomer	$E_{\text{H-L}}^{\text{HSE}}$ (eV)	LUMO (eV)	U_e (V)	$\Delta E_{*\text{COO}}$ (eV)
Pd_2S_2	1	1.51	-3.94	-0.16	-0.34
	2	1.35	-3.92	-0.14	-0.84
	3	1.26	-3.96	-0.18	-0.19
	4	1.34	-4.11	-0.33	-0.43
Pd_2S_3	1	2.06	-3.43	0.35	-0.98
	2	1.74	-4.52	-0.74	-0.23
	3	1.65	-4.51	-0.73	-0.37
	4	1.42	-4.51	-0.73	-0.34
	5	1.56	-3.43	0.35	-0.33
	6	1.44	-4.52	-0.74	-0.32
Pd_2S_4	1	1.92	-3.51	0.26	-0.82
	2	1.77	-4.01	-0.23	-0.53
	3	1.71	-4.04	-0.26	-0.98
	4	1.61	-3.90	-0.12	-1.39
	5	1.98	-3.50	0.28	-0.34
	6	1.35	-4.58	-0.80	-0.21
Pd_2S_8	1	2.40	-3.38	0.40	-0.24
	2	2.55	-3.16	0.62	—
	3	2.33	-3.36	0.42	—
	4	2.34	-3.12	0.66	—
	5	1.78	-3.21	0.57	—
Pd_3S_3	1	2.13	-2.93	0.85	-0.58
	2	1.05	-4.85	-1.07	-1.12
	3	1.05	-4.85	-1.07	-0.32
	4	1.06	-4.94	-1.16	-0.31
	5	1.47	-4.32	-0.54	-0.24
	6	1.25	-5.11	-1.33	-0.35
	7	1.23	-4.98	-1.20	-0.16
Pd_3S_4	1	1.80	-3.88	-0.10	-0.59
	2	2.03	-3.67	0.11	-0.94
	3	2.02	-3.67	0.11	-0.15
	4	1.57	-4.22	-0.44	-0.77
	5	1.60	-3.83	-0.05	-0.26
	6	1.82	-3.51	0.27	-0.23
	7	1.84	-3.36	0.42	-0.24
	1	1.91	-2.79	0.99	-0.46
	2	1.69	-4.14	-0.36	-0.03
	3	1.47	-4.49	-0.71	-1.07

Pd_3S_5	4	1.71	-4.09	-0.31	-0.22
	5	1.82	-4.03	-0.25	-0.47
	6	1.75	-3.87	-0.09	-0.25
	7	1.07	-5.11	-1.33	-0.25
Pd_3S_6	1	2.58	-2.75	1.03	-0.51
	2	1.72	-4.26	-0.48	-0.49
	3	1.56	-4.16	-0.38	-0.25
	4	2.08	-3.46	0.32	-0.56
	5	1.94	-3.67	0.11	-0.34
	6	1.78	-3.83	-0.05	-0.23
	7	1.56	-3.74	0.04	-0.17
Pd_4S_2	1	1.46	-3.91	-0.13	-0.32
	2	1.43	-3.70	-0.08	-0.70
	3	1.47	-3.99	-0.21	-0.12
	4	1.42	-4.01	-0.23	—
	5	0.89	-4.31	-0.53	—
	6	0.89	-4.32	-0.54	—
	7	0.80	-5.11	-1.33	—
Pd_4S_4	1	1.91	-3.64	0.14	-0.24
	2	1.27	-4.71	-0.93	-0.84
	3	1.69	-3.84	-0.06	-0.28
	4	1.53	-3.82	-0.04	-0.17
	5	1.87	-3.38	0.40	-0.24
	6	1.59	-3.93	-0.15	-0.24
	7	1.67	-3.46	0.32	-0.06
Pd_4S_5	1	1.87	-3.66	0.12	-0.45
	2	2.08	-3.43	0.35	—
	3	2.06	-3.44	0.34	-0.28
	4	1.76	-3.90	-0.12	—
	5	1.84	-3.68	0.10	—
	6	1.40	-4.75	-0.97	—
	7	1.70	-3.65	0.13	-0.50
Pd_4S_6	1	1.79	-3.29	0.49	-0.46
	2	2.32	-3.63	0.15	-0.47
	3	2.38	-2.79	0.79	-0.44
	4	1.80	-3.81	-0.03	-0.61
	5	1.89	-3.63	0.15	—
	6	1.63	-3.30	-0.58	—
	7	1.45	-3.45	-0.33	—
Pd_4S_7	1	2.17	-2.67	1.11	-0.57
	2	1.95	-3.68	0.10	-0.23
	3	1.81	-3.97	-0.19	-0.23
	4	2.19	-3.66	0.12	-0.31
	5	1.94	-3.78	0.00	-0.23
	6	2.13	-3.40	0.38	-0.48

	7	1.87	-3.84	-0.06	—
Pd_4S_8	1	2.80	-2.64	1.14	—
	2	2.39	-3.43	0.35	—
	3	2.34	-3.09	0.69	—
	4	2.19	-3.24	0.54	—
	5	1.81	-4.06	-0.28	—
	6	1.91	-3.68	0.10	-0.56
	7	1.78	-3.98	-0.20	-0.22
Pd_4S_{10}	1	2.33	-3.47	0.31	—
	2	2.39	-3.15	0.63	—
	3	2.02	-4.06	-0.28	—
	4	1.82	-3.78	0.00	—
	5	1.78	-4.03	-0.25	—
	6	1.64	-3.60	0.18	—
	7	1.53	-3.98	-0.20	—
Pd_5S_5	1	1.83	-3.20	0.58	-0.46
	2	1.63	-3.65	0.13	-0.55
	3	1.99	-3.25	0.53	—
	4	1.65	-3.97	-0.19	—
	5	1.95	-3.36	0.42	-0.36
	6	1.95	-3.39	0.39	-0.59
	7	1.60	-4.04	-0.26	-0.47
Pd_5S_6	1	1.78	-3.60	0.18	-0.70
	2	1.92	-3.61	0.17	—
	3	1.41	-4.68	-0.90	-0.29
	4	1.87	-3.55	0.23	-0.31
	5	1.94	-3.58	0.20	-0.24
	6	1.60	-3.93	-0.15	-0.23
	7	1.65	-3.86	-0.08	-0.44
Pd_5S_7	1	1.97	-3.35	0.43	-0.51
	2	1.92	-3.61	0.17	-0.44
	3	2.37	-3.05	0.73	-0.24
	4	1.21	-5.18	-1.40	-0.24
	5	1.76	-3.85	-0.07	-0.24
	6	1.95	-3.93	-0.15	-0.43
	7	1.67	-4.06	-0.28	-0.22
Pd_5S_8	1	2.29	-3.47	0.31	-0.22
	2	1.98	-3.68	0.10	-0.66
	3	2.22	-3.27	0.51	-0.24
	4	2.04	-3.52	0.26	—
	5	2.45	-2.88	0.90	-0.20
	6	2.16	-3.27	0.51	—
	7	2.03	-3.65	0.13	—
	1	1.85	-3.49	0.29	-0.58
	2	2.20	-3.29	0.49	—

Pd_5S_9	3	2.18	-3.61	0.17	—
	4	2.33	-3.19	0.59	—
	5	2.09	-3.60	0.18	—
	6	2.26	-3.32	0.46	—
	7	2.19	-3.49	0.29	—
Pd_5S_{10}	1	2.77	-3.36	0.42	—
	2	2.19	-3.32	0.46	—
	3	2.14	-3.42	0.36	—
	4	2.08	-3.84	-0.06	—
	5	2.07	-3.79	-0.01	—
	6	1.97	-3.97	-0.19	—
	7	1.95	-3.81	-0.03	—
Pd_6S_4	1	1.70	-3.94	-0.16	-0.28
	2	1.93	-3.52	0.26	-0.52
	3	1.54	-3.92	-0.14	-0.16
	4	1.70	-3.56	0.22	-0.19
	5	1.88	-3.24	0.54	-0.54
	6	1.53	-3.82	-0.04	-0.52
	7	1.73	-3.43	0.35	-0.04
Pd_6S_5	1	2.04	-3.74	0.04	—
	2	1.86	-3.77	0.01	—
	3	1.89	-3.78	0.00	—
	4	1.69	-3.91	-0.13	—
	5	1.78	-3.99	-0.21	—
	6	1.98	-4.07	-0.29	—
	7	1.52	-4.31	-0.53	—
Pd_6S_6	1	1.79	-3.35	0.43	-0.47
	2	1.67	-4.02	-0.24	—
	3	1.59	-4.06	-0.28	—
	4	1.56	-4.07	-0.29	—
	5	1.99	-3.34	0.44	—
	6	1.54	-4.45	-0.67	—
	7	1.42	-4.21	-0.43	—
Pd_6S_7	1	1.27	-5.14	-1.36	—
	2	2.01	-3.62	0.16	—
	3	1.48	-4.57	-0.79	—
	4	1.78	-3.91	-0.13	—
	5	2.20	-3.13	0.65	—
	6	1.05	-5.35	-1.57	—
	7	1.65	-3.91	-0.13	—
Pd_6S_8	1	2.10	-3.59	0.19	-0.73
	2	2.06	-3.48	0.30	-0.24
	3	1.99	-3.63	0.15	-0.02
	4	1.98	-3.76	0.02	-0.24
	5	1.91	-3.76	0.02	-0.25

	6	1.81	-4.00	-0.22	-0.24
	7	1.79	-4.13	-0.35	-0.73
Pd_6S_9	1	1.98	-4.07	-0.29	-0.24
	2	2.04	-3.74	0.04	-0.34
	3	2.09	-3.68	0.10	-0.26
	4	2.10	-3.55	0.23	-0.19
	5	1.52	-4.31	-0.53	-0.13
	6	2.17	-3.46	0.32	-0.25
	7	2.11	-3.41	0.37	-0.37
Pd_6S_{10}	1	0.76	-6.54	-2.76	-0.29
	2	2.07	-3.79	-0.01	-0.72
	3	2.08	-3.84	-0.06	-0.52
	4	1.97	-3.97	-0.19	-0.29
	5	2.20	-3.59	0.19	-0.26
	6	2.46	-2.96	0.82	—
	7	1.81	-4.10	-0.32	—
Pd_6S_{11}	1	2.35	-3.27	0.51	—
	2	2.39	-3.31	0.47	—
	3	2.34	-3.33	0.45	—
	4	2.31	-3.37	0.41	—
	5	2.09	-3.72	0.06	—
	6	2.14	-3.83	-0.05	—
	7	1.90	-4.02	-0.24	—
Pd_6S_{12}	1	2.71	-2.78	1.00	-0.21
	2	2.39	-3.31	0.47	-0.23
	3	2.45	-3.16	0.62	-0.21
	4	2.37	-3.32	0.46	-0.31
	5	2.41	-3.32	0.46	-0.22
	6	2.49	-2.87	0.91	-0.21
	7	1.90	-4.05	-0.27	-0.24
Pd_7S_5	1	1.35	-4.33	-0.55	-0.80
	2	1.28	-4.35	-0.57	-0.27
	3	1.55	-4.09	-0.31	-0.23
	4	1.41	-4.25	-0.47	-0.24
	5	1.46	-4.33	-0.55	-0.28
	6	1.16	-4.71	-0.93	-0.69
	7	1.38	-4.24	-0.46	-0.25
Pd_7S_6	1	1.49	-4.09	-0.31	—
	2	1.41	-4.25	-0.47	—
	3	1.32	-4.32	-0.54	—
	4	1.35	-4.33	-0.55	—
	5	1.46	-4.33	-0.55	—
	6	1.28	-4.35	-0.57	—
	7	1.16	-4.71	-0.93	—
	1	1.82	-3.75	0.03	-0.13

Pd_7S_7	2	1.80	-3.91	-0.13	-0.63
	3	1.80	-3.80	-0.02	-0.70
	4	1.51	-4.06	-0.28	-0.32
	5	1.28	-5.28	-1.50	-0.02
	6	1.27	-4.92	-1.14	-0.24
	7	1.17	-4.86	-1.08	-0.27
Pd_7S_8	1	1.75	-3.99	-0.21	—
	2	1.62	-4.13	-0.35	—
	3	1.61	-4.35	-0.57	—
	4	1.59	-4.32	-0.54	—
	5	1.43	-4.93	-1.15	—
	6	1.28	-5.16	-1.38	—
	7	1.17	-5.78	-2.00	—
Pd_7S_9	1	2.04	-3.47	0.31	—
	2	1.86	-4.09	-0.31	—
	3	1.84	-4.14	-0.36	—
	4	1.78	-4.26	-0.48	—
	5	1.72	-3.91	-0.13	—
	6	1.45	-5.20	-1.42	—
	7	1.27	-5.16	-1.38	—
Pd_7S_{10}	1	2.10	-3.63	0.15	—
	2	2.06	-3.77	0.01	—
	3	1.97	-3.90	-0.12	—
	4	1.87	-4.09	-0.31	—
	5	1.71	-4.27	-0.49	—
	6	1.49	-5.08	-1.30	—
	7	0.97	-6.07	-2.29	—
Pd_7S_{11}	1	2.13	-3.58	0.20	—
	2	2.11	-3.72	0.06	—
	3	2.08	-3.51	0.27	—
	4	1.94	-3.73	0.05	—
	5	1.83	-3.95	-0.17	—
	6	1.74	-4.35	-0.57	—
	7	1.04	-6.11	-2.33	—
Pd_7S_{12}	1	2.44	-3.09	0.69	—
	2	2.27	-3.49	0.29	—
	3	2.21	-3.70	0.08	—
	4	2.04	-3.60	0.18	—
	5	1.99	-3.59	0.19	—
	6	1.97	-3.90	-0.12	—
	7	1.59	-4.50	-0.72	—
Pd_8S_2	1	1.82	-3.33	0.45	—
	2	1.72	-4.11	-0.33	—
	3	1.64	-3.62	0.16	—
	4	1.64	-3.64	0.14	—

	5	1.50	-3.85	-0.07	—
	6	1.50	-3.84	-0.06	—
	7	1.39	-4.27	-0.49	—
Pd_8S_4	1	1.65	-4.74	-0.96	-0.38
	2	1.55	-4.83	-1.05	-0.20
	3	1.55	-4.84	-1.06	-0.21
	4	1.49	-5.00	-1.22	-0.23
	5	1.41	-5.07	-1.29	-0.18
	6	1.19	-5.52	-1.74	—
	7	0.69	-6.28	-2.50	—
Pd_8S_6	1	1.39	-4.35	-0.57	—
	2	1.37	-4.39	-0.61	—
	3	1.35	-4.72	-0.94	—
	4	1.34	-4.62	-0.84	—
	5	1.33	-4.21	-0.43	—
	6	1.32	-4.62	-0.84	—
	7	1.27	-4.98	-1.20	—
Pd_8S_8	1	1.66	-3.96	-0.18	-0.42
	2	1.54	-4.39	-0.61	-0.23
	3	1.46	-4.72	-0.94	—
	4	1.46	-4.38	-0.60	-0.24
	5	1.35	-4.88	-1.10	—
	6	1.58	-4.37	-0.59	—
	7	1.41	-4.30	-0.52	—
Pd_8S_9	1	1.53	-4.50	-0.72	-0.22
	2	1.29	-5.25	-1.47	-0.23
	3	1.11	-5.71	-1.93	-0.22
	4	1.70	-4.04	-0.26	-0.23
	5	1.39	-4.52	-0.74	-0.26
	6	1.35	-5.09	-1.31	-0.36
	7	1.34	-4.61	-0.83	-0.22
Pd_8S_{10}	1	2.00	-3.66	0.12	-0.26
	2	2.06	-3.73	0.05	0.07
	3	1.82	-3.88	-0.10	-0.26
	4	1.85	-4.04	-0.26	-0.25
	5	1.75	-4.04	-0.26	-0.22
	6	1.61	-4.08	-0.30	-0.32
	7	1.72	-4.11	-0.33	-0.28
Pd_8S_{11}	1	2.13	-3.60	0.18	-0.26
	2	2.11	-3.67	0.11	-0.41
	3	2.01	-3.68	0.10	-0.25
	4	1.77	-3.99	-0.21	-0.22
	5	2.02	-4.00	-0.22	-0.23
	6	1.98	-4.06	-0.28	-0.21
	7	1.68	-4.34	-0.56	—

Pd_8S_{12}	1	2.16	-3.47	0.31	—
	2	2.05	-3.76	0.02	—
	3	1.81	-3.88	-0.10	—
	4	2.01	-3.91	-0.13	—
	5	1.87	-3.92	-0.14	—
	6	2.08	-3.99	-0.21	—
	7	1.90	-4.03	-0.25	—
Pd_8S_{16}	1	2.82	-2.74	1.04	-0.25
	2	2.54	-3.14	0.64	-0.40
	3	2.34	-3.54	0.24	—
	4	2.22	-3.61	0.17	—
	5	2.11	-3.68	0.10	—
	6	2.11	-3.68	0.10	—
	7	2.24	-3.69	0.09	—
Pd_9S_9	1	1.70	-3.95	-0.17	-0.25
	2	1.83	-4.01	-0.23	-0.01
	3	1.66	-4.06	-0.28	-0.23
	4	1.53	-4.08	-0.30	-0.38
	5	1.57	-4.18	-0.40	-0.92
	6	1.60	-4.28	-0.50	-0.28
	7	1.51	-4.36	-0.58	-0.37
Pd_9S_{10}	1	1.91	-3.94	-0.16	-0.18
	2	1.65	-4.00	-0.22	-0.23
	3	1.64	-4.15	-0.37	-0.24
	4	1.55	-4.29	-0.51	-0.21
	5	1.58	-4.31	-0.53	-0.33
	6	1.67	-4.31	-0.53	—
	7	1.40	-4.48	-0.70	—
Pd_9S_{11}	1	1.95	-3.75	0.03	0.97
	2	1.73	-3.94	-0.16	-1.38
	3	1.82	-3.99	-0.21	-0.87
	4	1.90	-4.01	-0.23	0.09
	5	1.83	-4.05	-0.27	0.08
	6	1.74	-4.05	-0.27	0.86
	7	1.76	-4.23	-0.45	-1.97
$Pd_{10}S_{10}$	1	1.78	-3.95	-0.17	—
	2	1.84	-3.96	-0.18	—
	3	1.84	-4.04	-0.26	—
	4	1.85	-4.04	-0.26	—
	5	1.56	-4.21	-0.43	—
	6	1.56	-4.21	-0.43	—
	7	1.52	-4.40	-0.62	—
	1	2.05	-4.14	-0.36	-0.22
	2	2.00	-4.15	-0.37	-0.38
	3	1.96	-4.22	-0.44	-0.20

$Pd_{10}S_{20}$	4	1.67	-4.28	-0.50	—
	5	1.55	-4.39	-0.61	—
	6	1.49	-4.41	-0.63	—
	7	1.72	-4.56	-0.78	—
$Pd_{12}S_{12}$	1	1.66	-4.41	-0.63	—
	2	1.59	-4.55	-0.77	—
	3	1.50	-4.54	-0.76	—
	4	1.50	-4.54	-0.76	—
	5	1.44	-4.64	-0.86	—
	6	1.43	-4.79	-1.01	—
	7	1.39	-4.40	-0.62	—

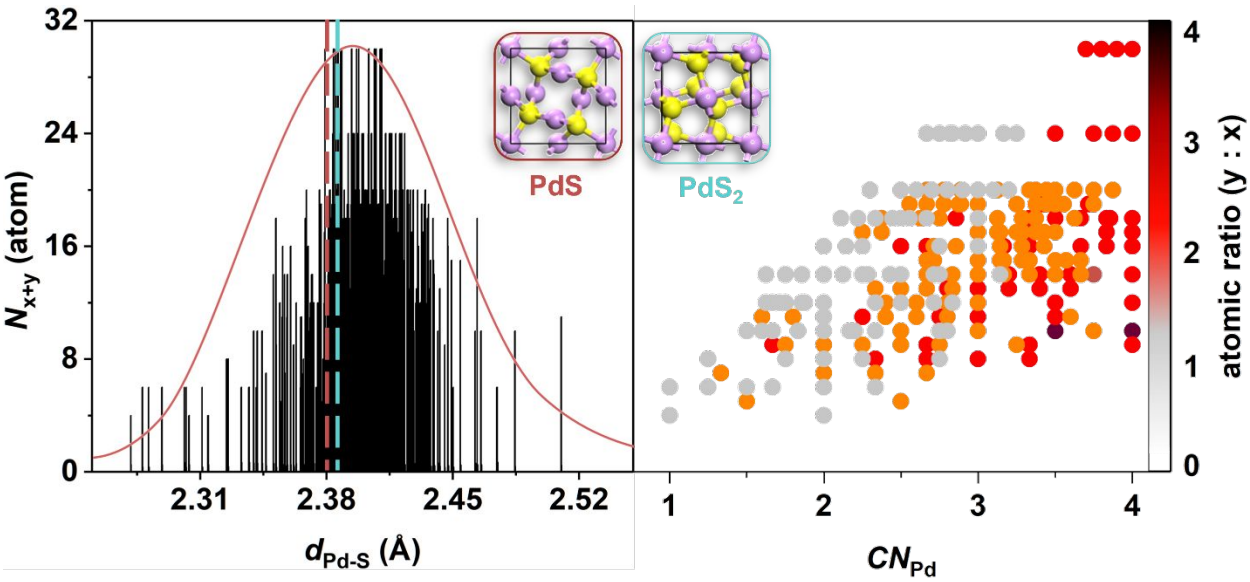

Figure S12. The total number of atoms vs. the average Pd−S bond length (left panel) and the avergae coordination number of Pd atoms (CN_{Pd}) in Pd_xS_y clusters ($x + y \leq 30$). The red and cycan dashed line indicates Pd−S bond length of bulk PdS and PdS_2, respectively. The color bar of the right axis shows the y : x atomic ratio of the clusters. The insets are the crystal structures of bulk PdS. The Pd and S atoms are shown in purple and yellow colors, respectively.

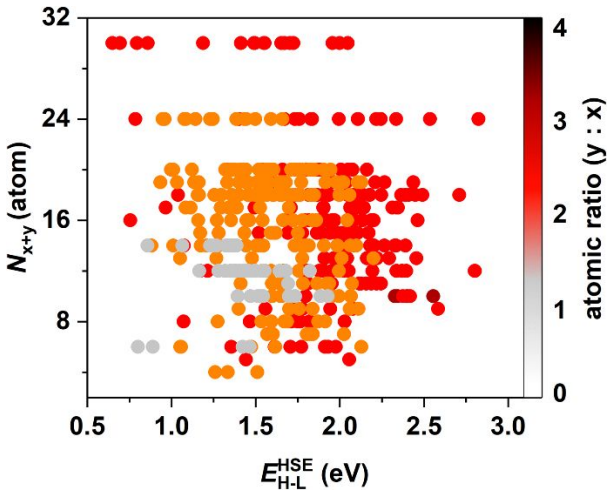

Figure S13. The total number of atoms vs. HOMO-LUMO gap of Pd_xS_y clusters ($x + y \leq 30$) calculated by the HSE06 functional. The color bar of the right axis shows the y : x atomic ratio of the clusters.

S4. Structure−activity relationship

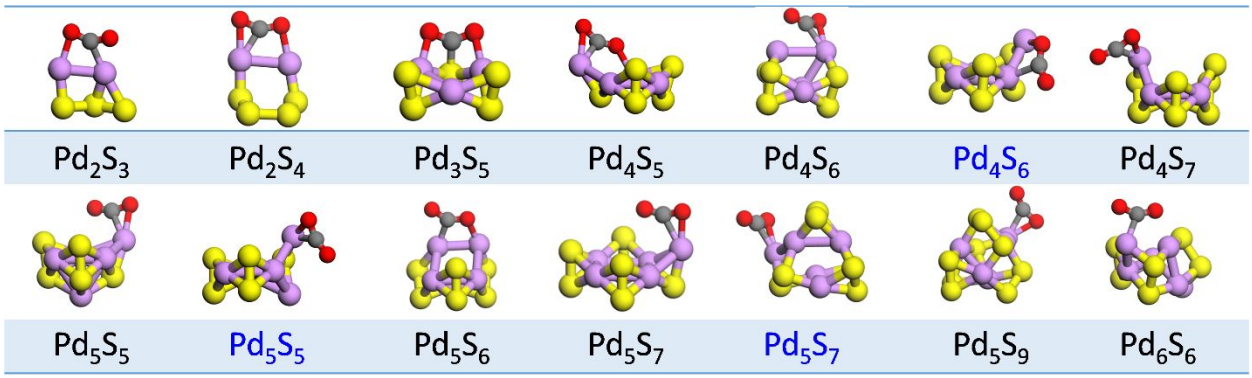

Figure S14. Atomic geometries of absorbed CO_2 on 14 candidate Pd_xS_y clusters. The C, O, S and Pd are shown in gray, red, yellow and purple colors, respectively. The Pd_xS_y clusters in the ground states are marked in black, and those metastable isomers are marked in blue.

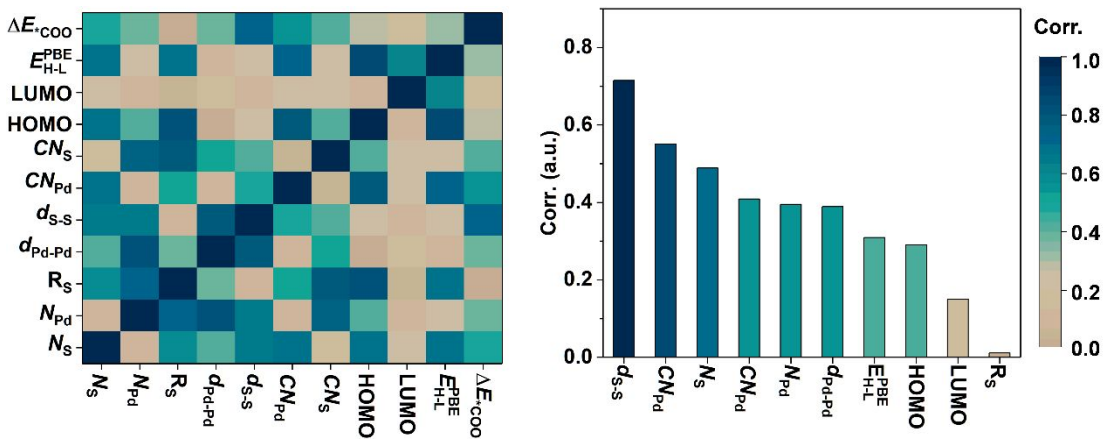

Figure S15. Left panel: heat map of the Pearson correlation coefficient (Corr.) matrix among the selected features for Pd_xS_y clusters. Right panel: histogram of correlation coefficient between CO_2 adsorption energy and various geometric/electronic features.

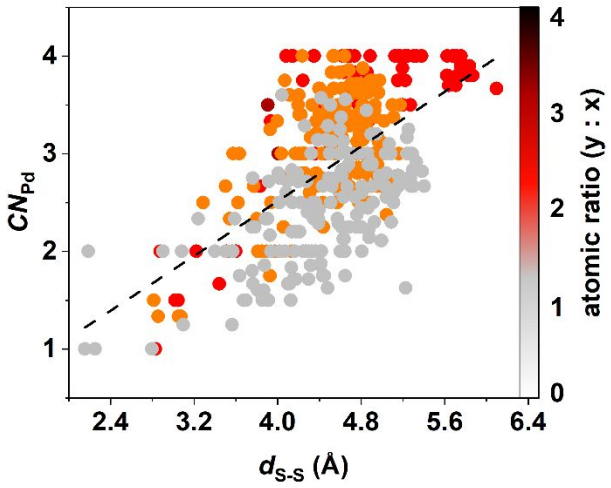

Figure S16. The avergae coordination number of Pd atoms (CN_{Pd}) vs. the average S−S distance (d_{S-S}) of Pd_xS_y clusters. The black dashed line is for visual aid.

S5. Candidate Pd_xS_y cluster catalysts for CO_2-HCOOH interconversion

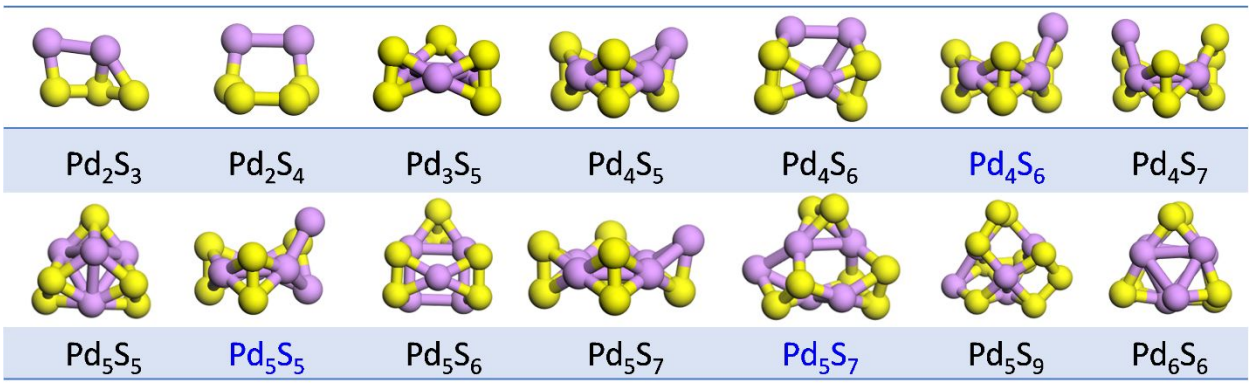

Figure S17. Atomic geometries of 14 candidate Pd_xS_y clusters. The S and Pd are shown in yellow and purple colors, respectively. The Pd_xS_y clusters in the ground states are marked in black, and those metastable isomers are marked in blue.

Table S4. The key parameters of screened 14 Pd_xS_y cluster catalysts, inlcuding relative total energy (E_{total}), formation energy (E_{form}), average coordination number of Pd atoms (CN_{Pd}), HOMO-LUMO gap ($E_{H\text{-}L}^{HSE}$), reduction power (U_e), bond length between Pd and C atom ($d_{Pd\text{-}C}$), Pd and O atom ($d_{Pd\text{-}O}$), and C and O atom ($d_{C\text{-}O}$), bond angle of bended *COO, and adsorption energies of chemisorbed CO_2 molecule. The Pd_xS_y clusters in the ground states are marked in black, and those metastable isomers are marked in blue.

system	E_{total} (eV)	E_{form} (eV)	CN_{pd}	$E_{H\text{-}L}^{HSE}$ (eV)	U_e (eV)	$d_{Pd\text{-}C}$ (Å)	$d_{Pd\text{-}O}$ (Å)	$d_{C\text{-}O}$ (Å)	α (°)	CT_{*COO} (e)	ΔE_{*COO} (eV)
Pd_2S_3	0	−1.85	2.5	2.06	0.32	2.09	2.24	1.24	144.48	0.35	−0.98
Pd_2S_4	0	−1.94	2	1.92	0.26	2.07	2.26	1.24	143.25	0.32	−0.82
Pd_3S_5	0	−2.14	2.3	1.91	0.99	2.45	2.19	1.27	130.46	0.54	−0.46
Pd_4S_5	0	−2.23	2.5	1.87	0.12	1.99	2.47	1.24	140.70	0.37	−0.45
Pd_4S_6	0	−2.33	2.3	1.79	0.47	2.11	2.22	1.22	147.08	0.28	−0.46
Pd_4S_6	+0.12	−2.11	2.4	2.32	0.15	2.29	2.17	1.20	146.10	0.32	−0.47
Pd_4S_7	0	−2.34	2.2	2.17	1.11	2.13	2.20	1.22	153.98	0.21	−0.57
Pd_5S_5	0	−2.26	2.8	1.83	0.58	2.15	2.22	1.21	153.94	0.21	−0.46
Pd_5S_5	+0.20	−2.13	2.2	1.63	0.13	2.16	2.21	1.22	153.07	0.23	−0.55
Pd_5S_6	0	−2.28	2.6	1.78	0.18	2.06	2.12	1.24	140.13	0.41	−0.70
Pd_5S_7	0	−2.42	2.8	1.97	0.43	2.22	2.21	1.21	155.96	0.17	−0.51
Pd_5S_7	+0.32	−2.22	2.4	1.92	0.17	2.20	2.25	1.20	157.00	0.16	−0.45
Pd_5S_9	0	−2.46	3.2	1.85	0.29	2.14	2.20	1.24	153.27	0.22	−0.58
Pd_6S_6	0	−2.40	2.4	1.79	0.43	2.04	2.37	1.23	147.44	0.31	−0.47

S6. Stability, activity and selectivity of Pd_xS_y clusters in aqueous environment

Table S5. Zero-point energy (ZPE) and entropic correction (*TS*) at *T* =298.15 K for the molecules and intermediate species involved in the CO_2 reduction to HCOOH on the Pd_4S_7 cluster. These values are close to the data of other candidate Pd_xS_y clusters, and thus are used throughout the calculation of free energy diagrams.

Species	ZPE (eV)	*TS* (eV)	ZPE–*TS* (eV)
H_2	0.29	0.41	–0.12
H_2O	0.60	0.59	0.01
CO	0.14	0.62	–0.48
CO_2	0.32	0.66	–0.34
HCOOH	0.92	1.02	–0.10
CO_2*	0.21	0.16	0.05
OOCH*	0.44	0.23	0.21
COOH*	0.46	0.14	0.31
CO*	0.13	0.08	0.05
HCOOH*	0.64	0.17	0.47

For gaseous molecules, the values of ZPE and *TS* are obtained from the NIST-JANAF thermochemical table.[5] Then, the Gibbs free energy of formation for each reaction step on the Pd_xS_y clusters is calculated as $\Delta G = \Delta E + \Delta ZPE - T\Delta S$ with ΔE, ΔZPE and ΔS representing the differences of the DFT total energy, zero-point energy and entropy between the initial and final states, respectively.

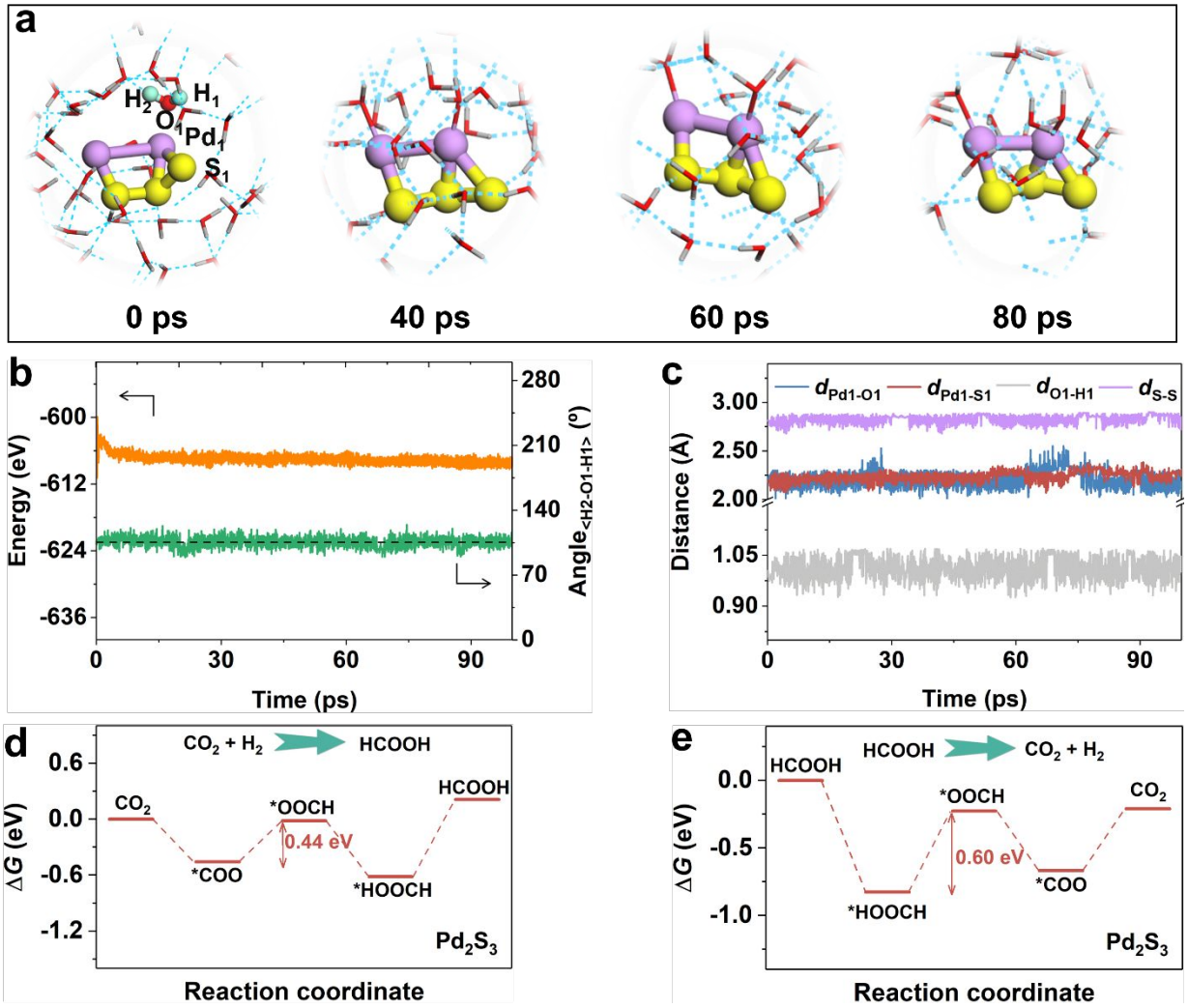

Figure S18. (**a**) Snapshots of the atomic structures of Pd_2S_3 cluster in water by AIMD simulations of 0, 40, 60 and 80 ps at 300K. The Pd, S, O, and H atoms are shown in purple, yellow, red, and light gray, respectively. The H atoms of H_2O in the nearest neighbor of Pd_2S_3 were shown in cyan for visual clarity. The hydrogen bonds are indicated by dashed cyan lines. (**b**) Time evolution of total energy (orange) and bond angle of the H_2O molecule in the nearest neighbor of Pd_2S_3 (green). The black dashed line shows the bond angle of free H_2O molecule. (**c**) Time evolution of representative interatomic distances in the Pd_2S_3 cluster and the nearest-neighboring H_2O molecule. The free energy diagrams of CO_2 reduction and HCOOH dehydrogenation process on (**d** and **e**) Pd_2S_3 in solvation media, respectively. The inset arrows and numbers indicate the rate-determining step and the corresponding Gibbs free energy to overcome.

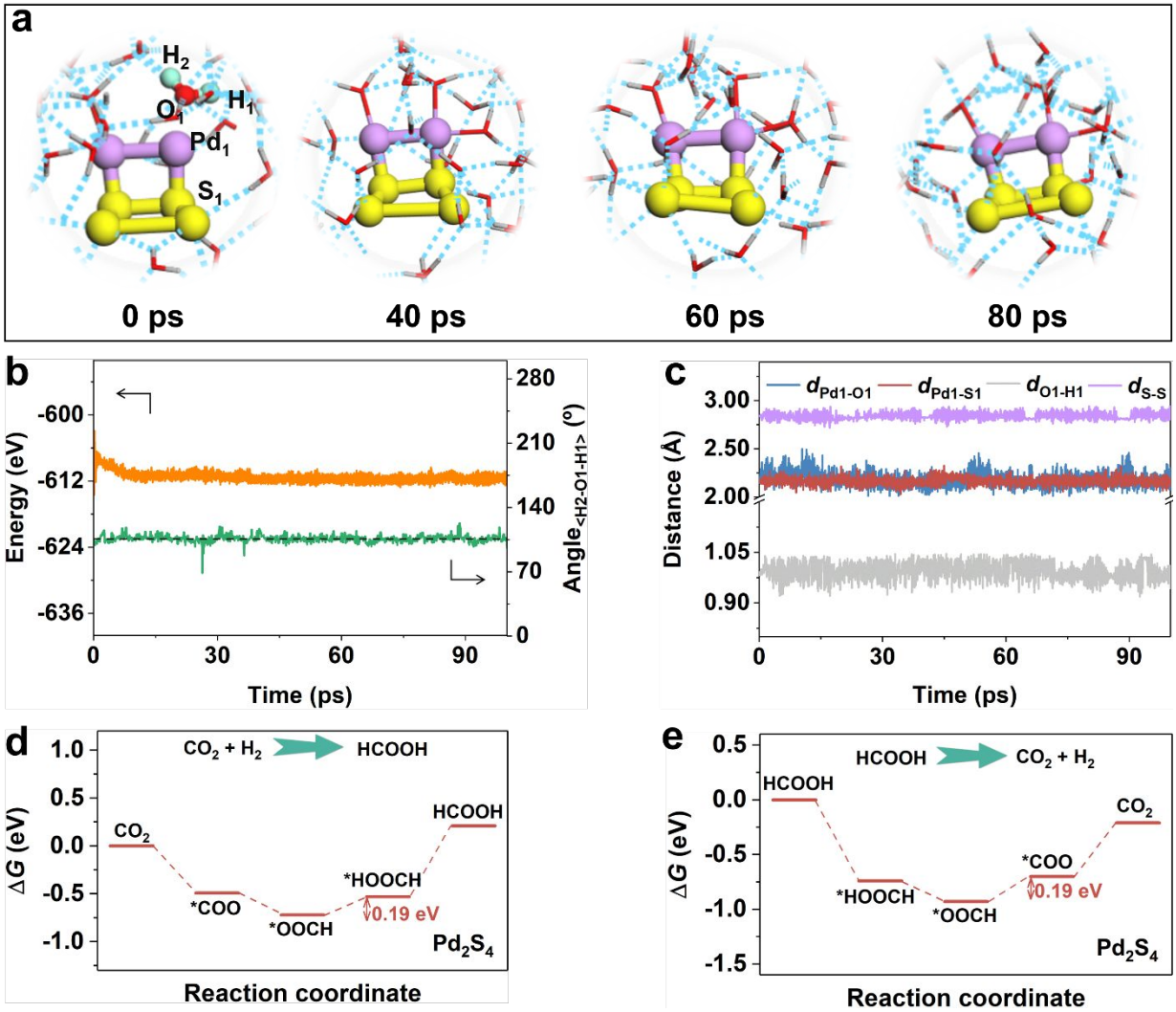

Figure S19. (**a**) Snapshots of the atomic structures of Pd_2S_4 cluster in water by AIMD simulations of 0, 40, 60 and 80 ps at 300K. The Pd, S, O, and H atoms are shown in purple, yellow, red, and light gray, respectively. The H atoms of H_2O in the nearest neighbor of Pd_2S_4 were shown in cyan for visual clarity. The hydrogen bonds are indicated by dashed cyan lines. (**b**) Time evolution of total energy (orange) and bond angle of the H_2O molecule in the nearest neighbor of Pd_2S_4 (green). The black dashed line shows the bond angle of free H_2O molecule. (**c**) Time evolution of representative interatomic distances in the Pd_2S_4 cluster and the nearest-neighboring H_2O molecule. The free energy diagrams of CO_2 reduction and HCOOH dehydrogenation process on (**d** and **e**) Pd_2S_4 in solvation media, respectively. The inset arrows and numbers indicate the rate-determining step and the corresponding Gibbs free energy to overcome.

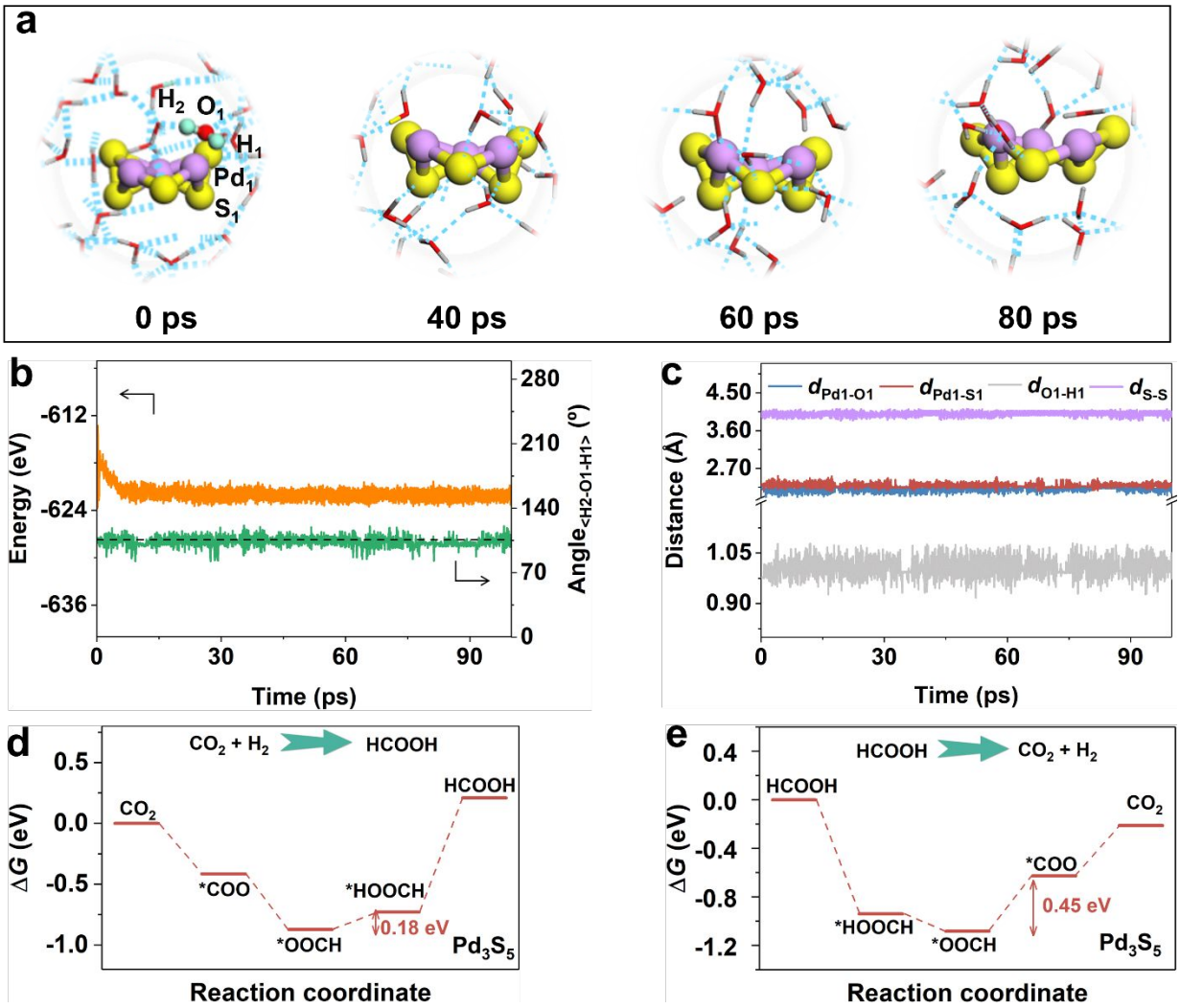

Figure S20. (**a**) Snapshots of the atomic structures of Pd_3S_5 cluster in water by AIMD simulations of 0, 40, 60 and 80 ps at 300K. The Pd, S, O, and H atoms are shown in purple, yellow, red, and light gray, respectively. The H atoms of H_2O in the nearest neighbor of Pd_3S_5 were shown in cyan for visual clarity. The hydrogen bonds are indicated by dashed cyan lines. (**b**) Time evolution of total energy (orange) and bond angle of the H_2O molecule in the nearest neighbor of Pd_3S_5 (green). The black dashed line shows the bond angle of free H_2O molecule. (**c**) Time evolution of representative interatomic distances in the Pd_3S_5 cluster and the nearest-neighboring H_2O molecule. The free energy diagrams of CO_2 reduction and HCOOH dehydrogenation process on (**d** and **e**) Pd_3S_5 in solvation media, respectively. The inset arrows and numbers indicate the rate-determining step and the corresponding Gibbs free energy to overcome.

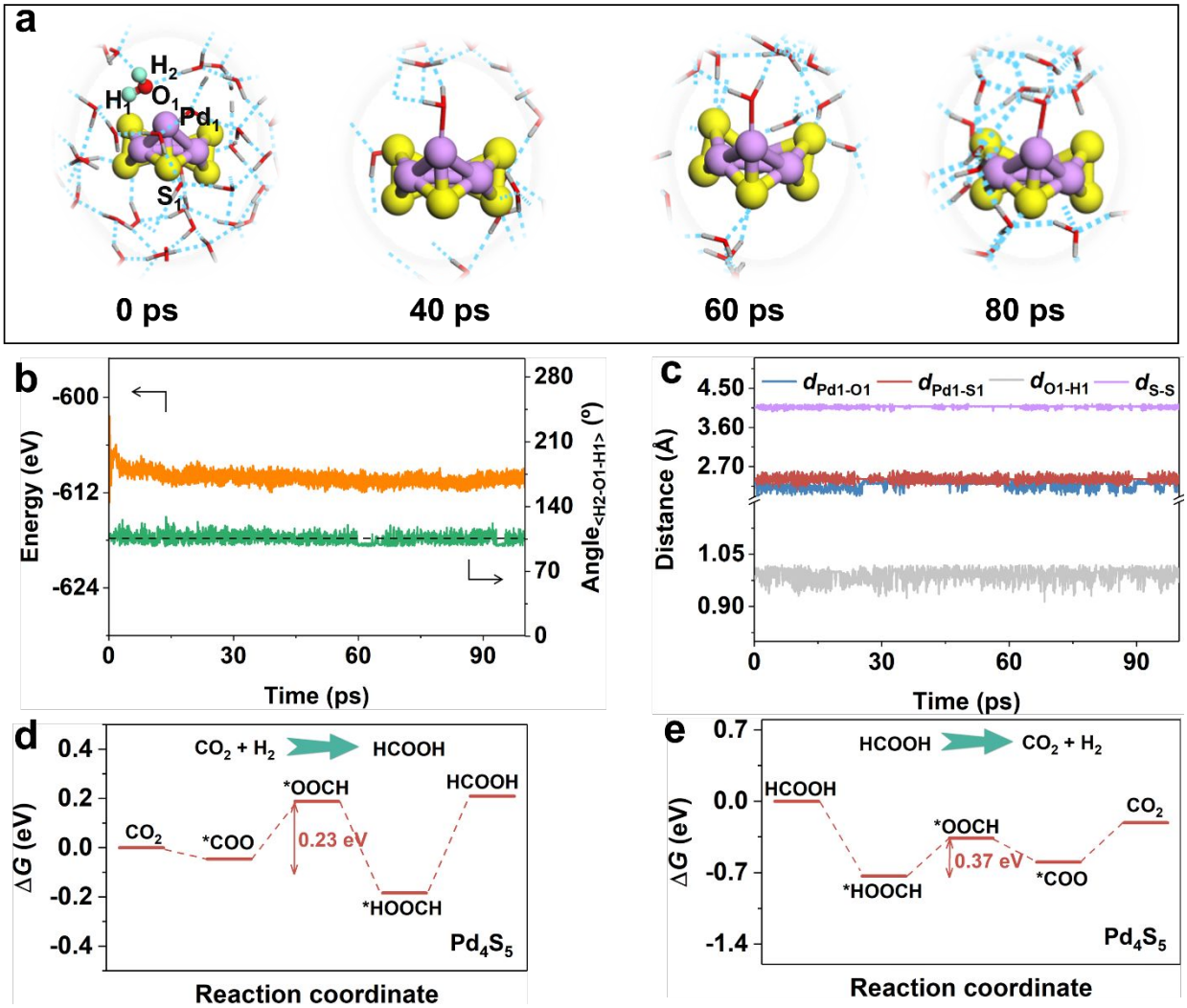

Figure S21. (**a**) Snapshots of the atomic structures of Pd_4S_5 cluster in water by AIMD simulations of 0, 40, 60 and 80 ps at 300K. The Pd, S, O, and H atoms are shown in purple, yellow, red, and light gray, respectively. The H atoms of H_2O in the nearest neighbor of Pd_4S_5 were shown in cyan for visual clarity. The hydrogen bonds are indicated by dashed cyan lines. (**b**) Time evolution of total energy (orange) and bond angle of the H_2O molecule in the nearest neighbor of Pd_4S_5 (green). The black dashed line shows the bond angle of free H_2O molecule. (**c**) Time evolution of representative interatomic distances in the Pd_4S_5 cluster and the nearest-neighboring H_2O molecule. The free energy diagrams of CO_2 reduction and HCOOH dehydrogenation process on (**d** and **e**) Pd_4S_5 in solvation media, respectively. The inset arrows and numbers indicate the rate-determining step and the corresponding Gibbs free energy to overcome.

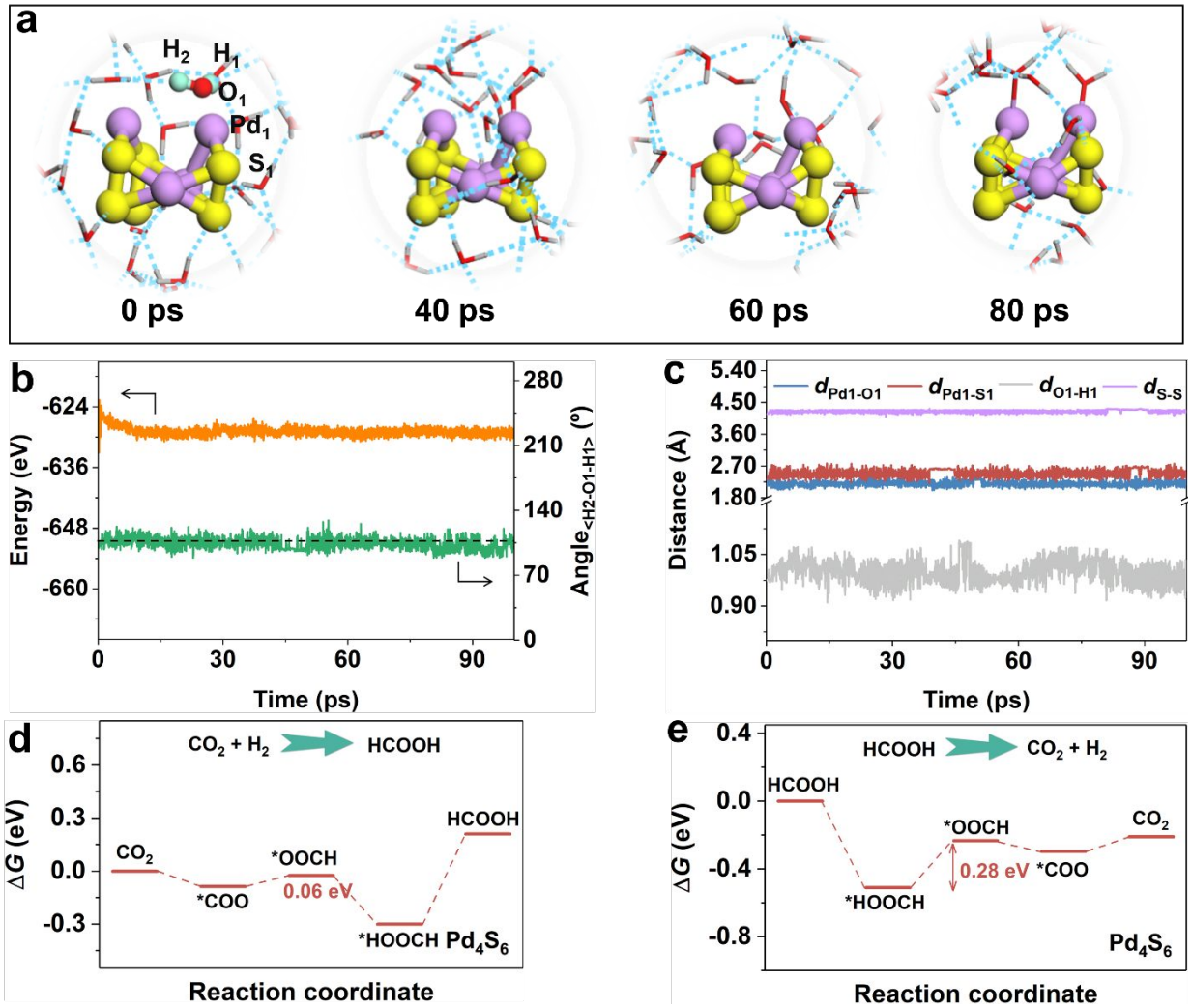

Figure S22. (**a**) Snapshots of the atomic structures of ground-state Pd_4S_6 cluster in water by AIMD simulations of 0, 40, 60 and 80 ps at 300K. The Pd, S, O, and H atoms are shown in purple, yellow, red, and light gray, respectively. The H atoms of H_2O in the nearest neighbor of ground-state Pd_4S_6 were shown in cyan for visual clarity. The hydrogen bonds are indicated by dashed cyan lines. (**b**) Time evolution of total energy (orange) and bond angle of the H_2O molecule in the nearest neighbor of ground-state Pd_4S_6 (green). The black dashed line shows the bond angle of free H_2O molecule. (**c**) Time evolution of representative interatomic distances in the ground-state Pd_4S_6 cluster and the nearest-neighboring H_2O molecule. The free energy diagrams of CO_2 reduction and HCOOH dehydrogenation process on (**d** and **e**) ground-state Pd_4S_6 in solvation media, respectively. The inset arrows and numbers indicate the rate-determining step and the corresponding Gibbs free energy to overcome.

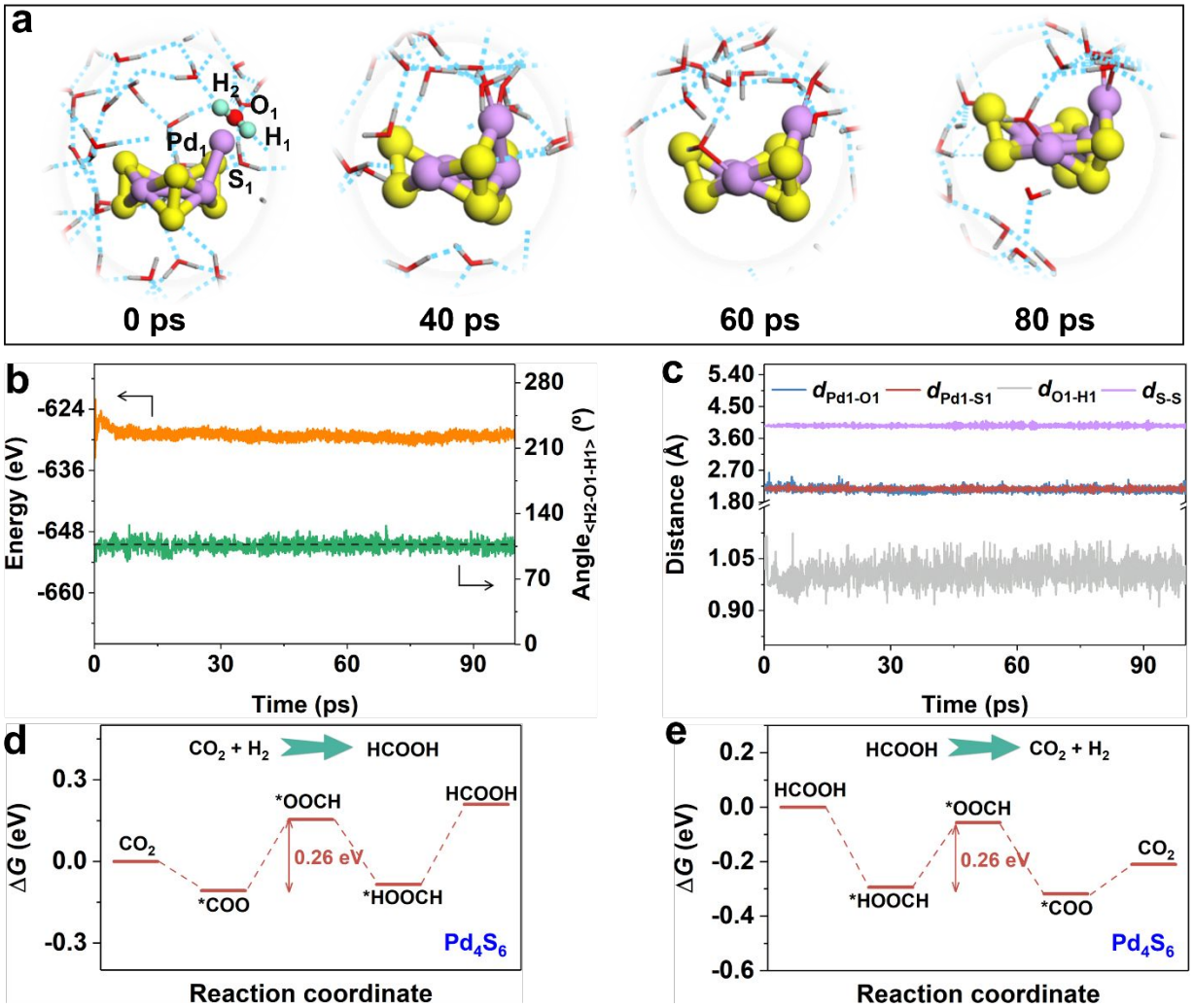

Figure S23. (**a**) Snapshots of the atomic structures of metastable Pd_4S_6 cluster in water by AIMD simulations of 0, 40, 60 and 80 ps at 300K. The Pd, S, O, and H atoms are shown in purple, yellow, red, and light gray, respectively. The H atoms of H_2O in the nearest neighbor of metastable Pd_4S_6 were shown in cyan for visual clarity. The hydrogen bonds are indicated by dashed cyan lines. (**b**) Time evolution of total energy (orange) and bond angle of the H_2O molecule in the nearest neighbor of metastable Pd_4S_6 (green). The black dashed line shows the bond angle of free H_2O molecule. (**c**) Time evolution of representative interatomic distances in the metastable Pd_4S_6 cluster and the nearest-neighboring H_2O molecule. The free energy diagrams of CO_2 reduction and HCOOH dehydrogenation process on (**d** and **e**) metastable Pd_4S_6 in solvation media, respectively. The inset arrows and numbers indicate the rate-determining step and the corresponding Gibbs free energy to overcome.

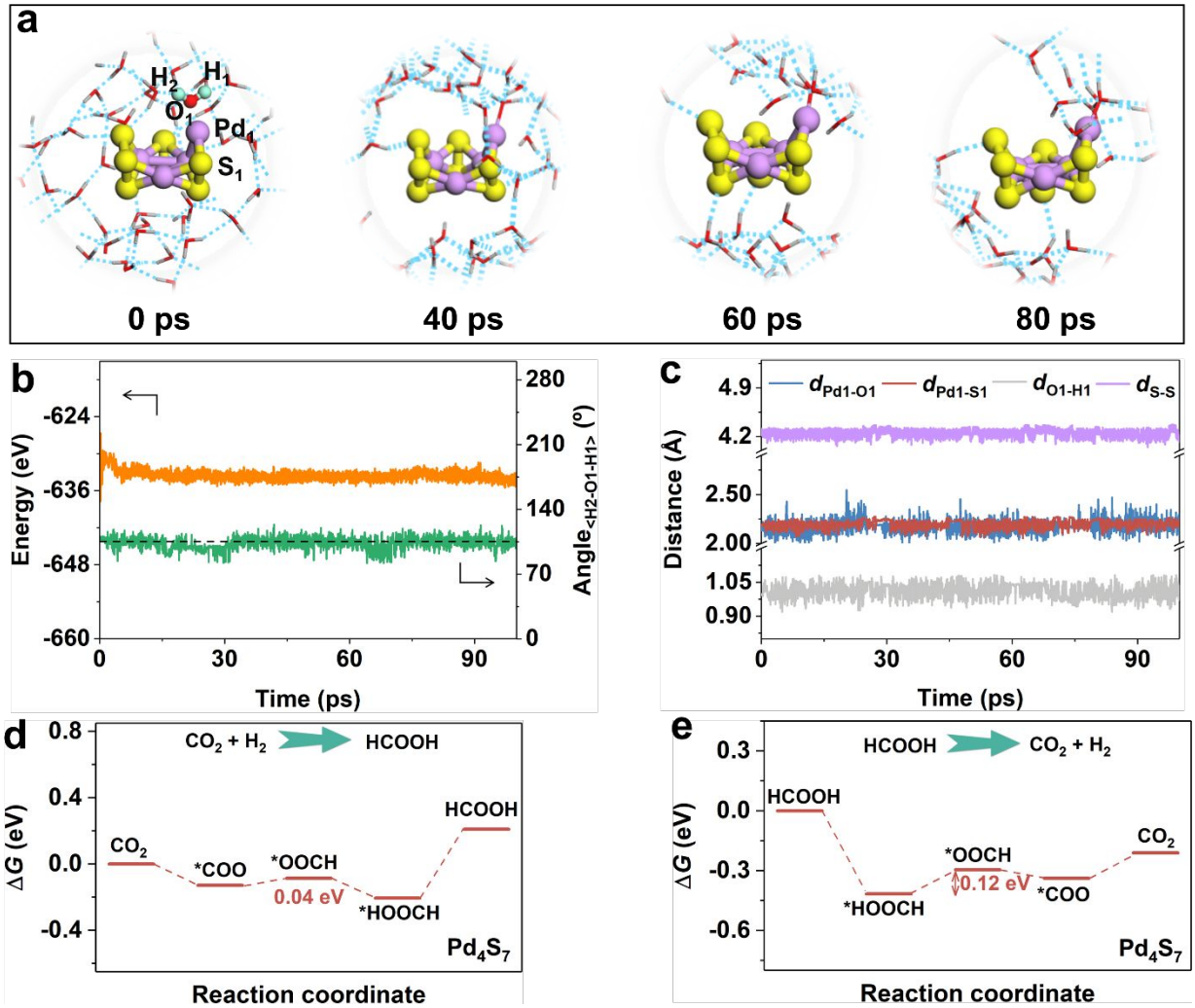

Figure S24. (**a**) Snapshots of the atomic structures of Pd_4S_7 cluster in water by AIMD simulations of 0, 40, 60 and 80 ps at 300K. The Pd, S, O, and H atoms are shown in purple, yellow, red, and light gray, respectively. The H atoms of H_2O in the nearest neighbor of Pd_4S_7 were shown in cyan for visual clarity. The hydrogen bonds are indicated by dashed cyan lines. (**b**) Time evolution of total energy (orange) and bond angle of the H_2O molecule in the nearest neighbor of ground-state Pd_5S_5 (green). The black dashed line shows the bond angle of free H_2O molecule. (**c**) Time evolution of representative interatomic distances in the Pd_4S_7 cluster and the nearest-neighboring H_2O molecule. The free energy diagrams of CO_2 reduction and HCOOH dehydrogenation process on (**d** and **e**) Pd_4S_7 in solvation media, respectively. The inset arrows and numbers indicate the rate-determining step and the corresponding Gibbs free energy to overcome.

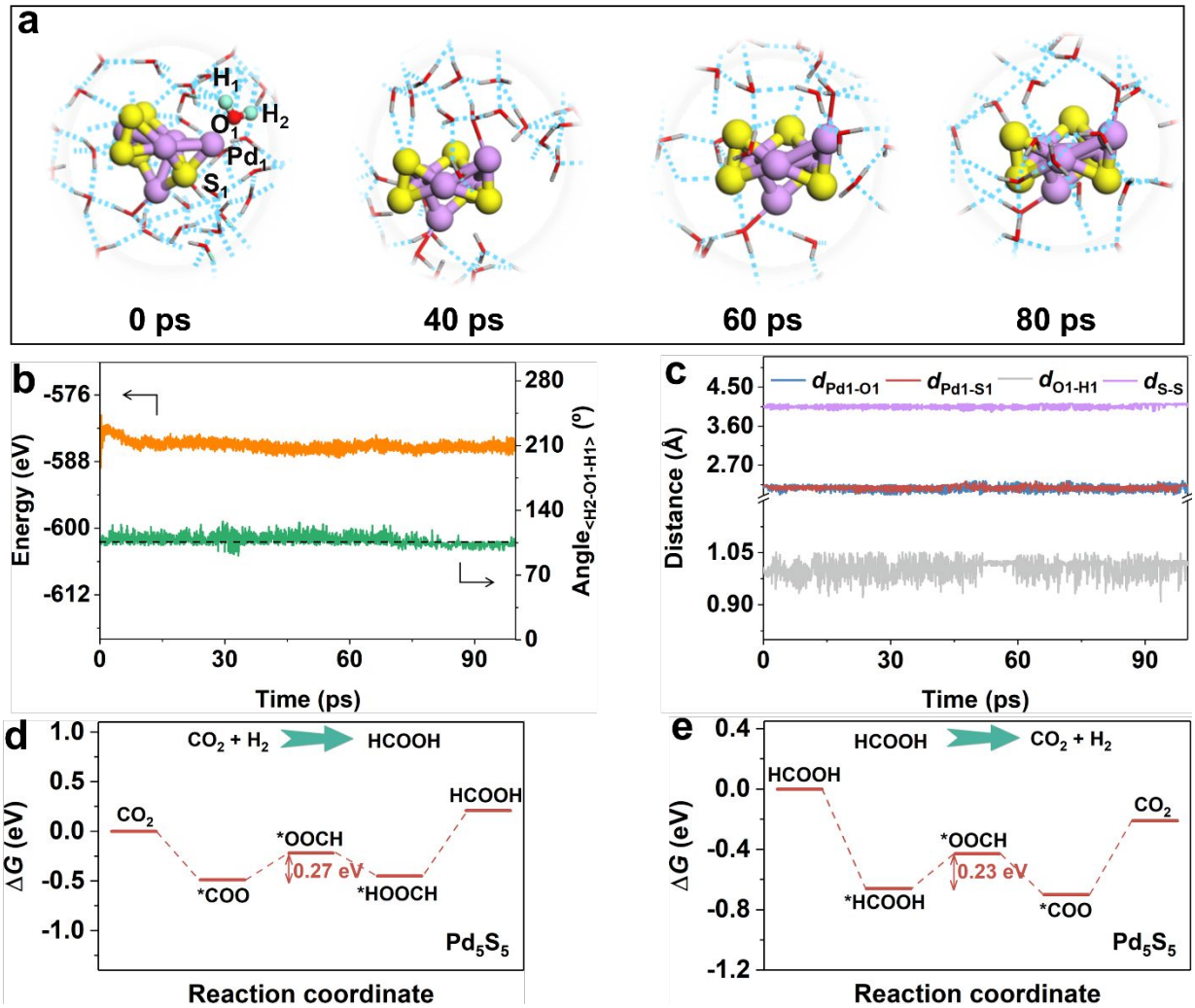

Figure S25. (**a**) Snapshots of the atomic structures of ground-state Pd_5S_5 cluster in water by AIMD simulations of 0, 40, 60 and 80 ps at 300K. The Pd, S, O, and H atoms are shown in purple, yellow, red, and light gray, respectively. The H atoms of H_2O in the nearest neighbor of ground-state Pd_5S_5 were shown in cyan for visual clarity. The hydrogen bonds are indicated by dashed cyan lines. (**b**) Time evolution of total energy (orange) and bond angle of the H_2O molecule in the nearest neighbor of ground-state Pd_5S_5 (green). The black dashed line shows the bond angle of free H_2O molecule. (**c**) Time evolution of representative interatomic distances in the ground-state Pd_5S_5 cluster and the nearest-neighboring H_2O molecule. The free energy diagrams of CO_2 reduction and HCOOH dehydrogenation process on (**d** and **e**) ground-state Pd_5S_5 in solvation media, respectively. The inset arrows and numbers indicate the rate-determining step and the corresponding Gibbs free energy to overcome.

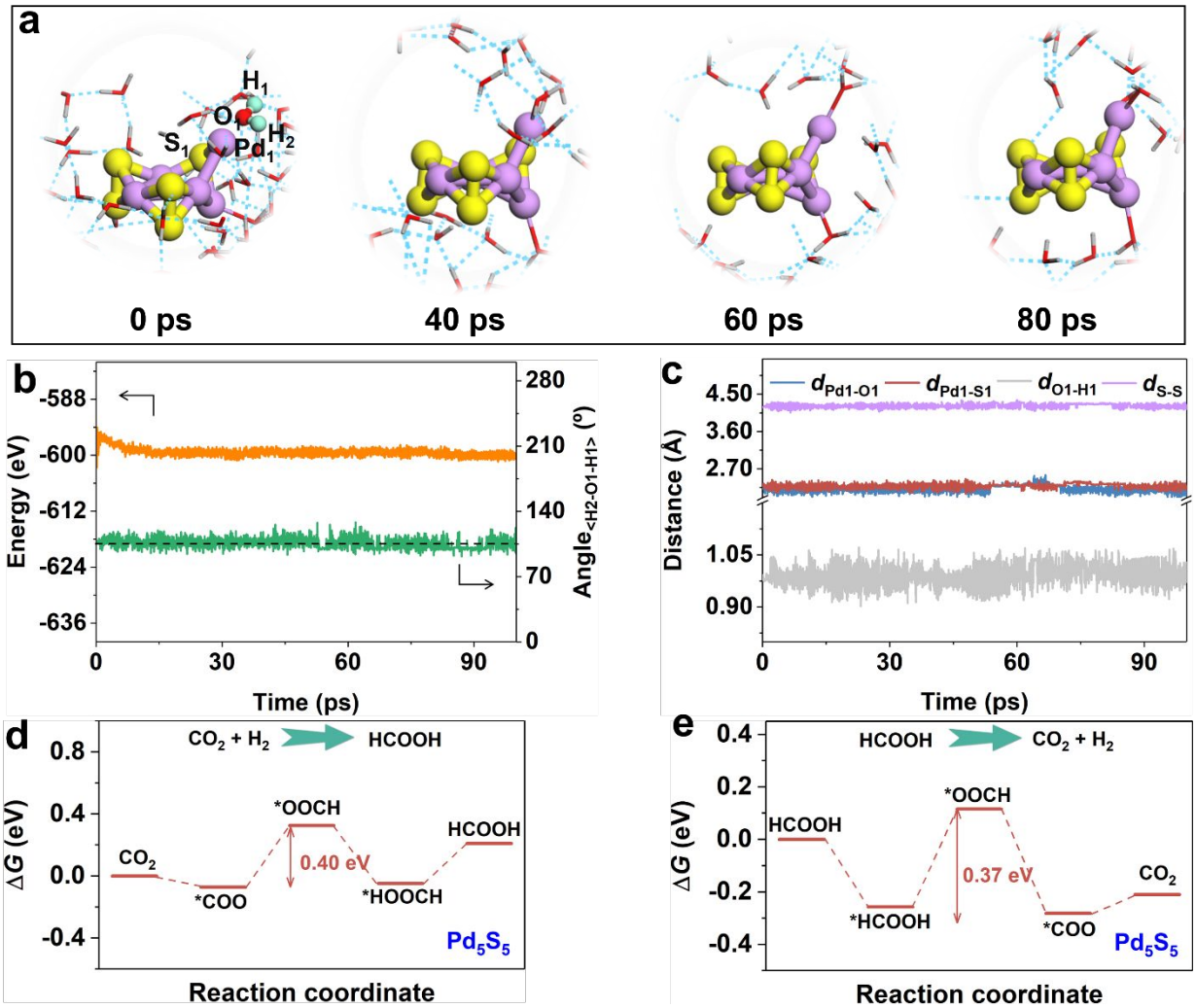

Figure S26. (**a**) Snapshots of the atomic structures of metastable Pd_5S_5 cluster in water by AIMD simulations of 0, 40, 60 and 80 ps at 300K. The Pd, S, O, and H atoms are shown in purple, yellow, red, and light gray, respectively. The H atoms of H_2O in the nearest neighbor of metastable Pd_5S_5 were shown in cyan for visual clarity. The hydrogen bonds are indicated by dashed cyan lines. (**b**) Time evolution of total energy (orange) and bond angle of the H_2O molecule in the nearest neighbor of metastable Pd_5S_5 (green). The black dashed line shows the bond angle of free H_2O molecule. (**c**) Time evolution of representative interatomic distances in the metastable Pd_5S_5 cluster and the nearest-neighboring H_2O molecule. The free energy diagrams of CO_2 reduction and HCOOH dehydrogenation process on (**d** and **e**) metastable Pd_5S_5 in solvation media, respectively. The inset arrows and numbers indicate the rate-determining step and the corresponding Gibbs free energy to overcome.

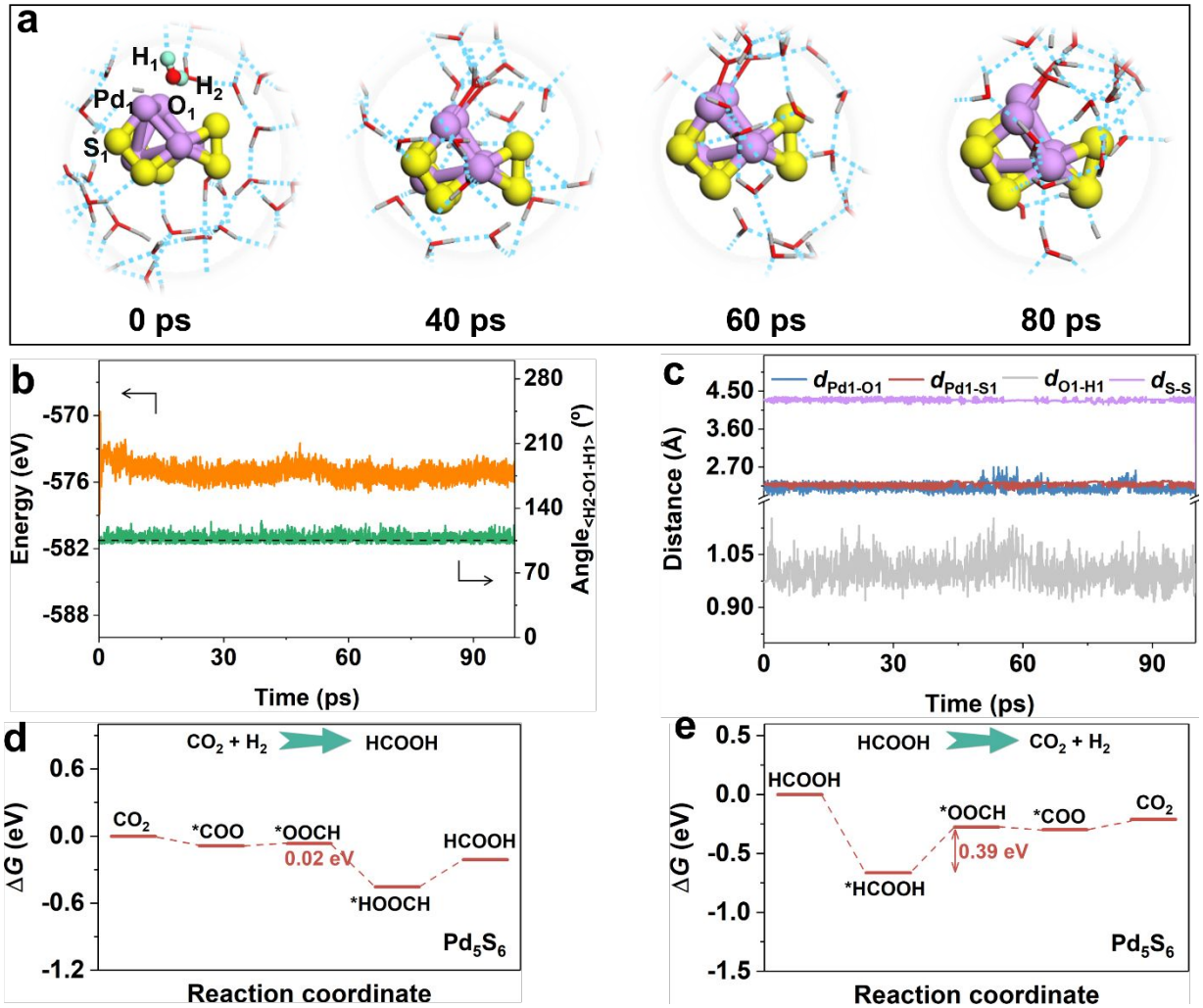

Figure S27. (**a**) Snapshots of the atomic structures of Pd_5S_6 cluster in water by AIMD simulations of 0, 40, 60 and 80 ps at 300K. The Pd, S, O, and H atoms are shown in purple, yellow, red, and light gray, respectively. The H atoms of H_2O in the nearest neighbor of Pd_5S_6 were shown in cyan for visual clarity. The hydrogen bonds are indicated by dashed cyan lines. (**b**) Time evolution of total energy (orange) and bond angle of the H_2O molecule in the nearest neighbor of Pd_5S_6 (green). The black dashed line shows the bond angle of free H_2O molecule. (**c**) Time evolution of representative interatomic distances in the Pd_5S_6 cluster and the nearest-neighboring H_2O molecule. The free energy diagrams of CO_2 reduction and HCOOH dehydrogenation process on (**d** and **e**) Pd_5S_6 in solvation media, respectively. The inset arrows and numbers indicate the rate-determining step and the corresponding Gibbs free energy to overcome.

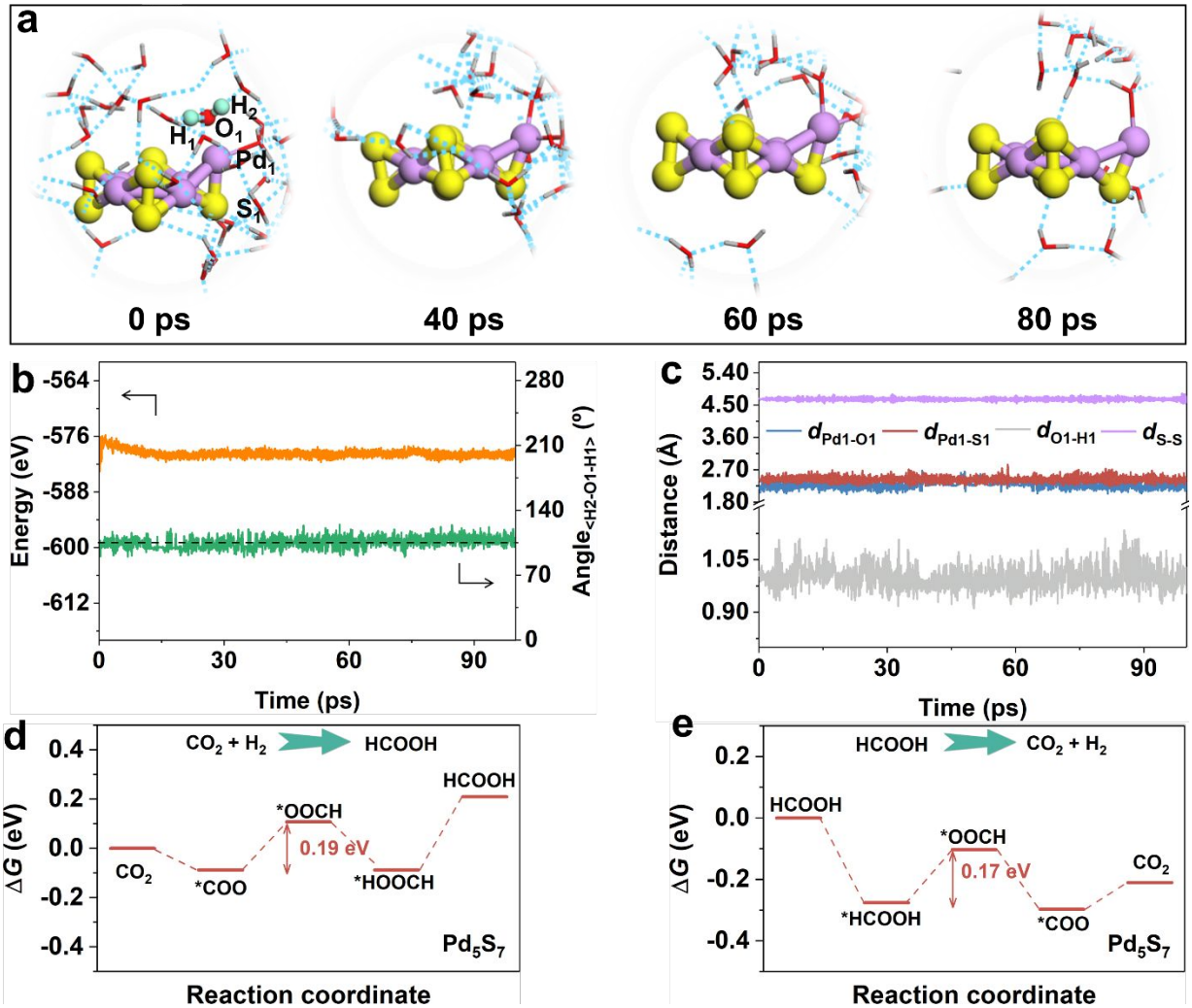

Figure S28. (**a**) Snapshots of the atomic structures of ground-state Pd_5S_7 cluster in water by AIMD simulations of 0, 40, 60 and 80 ps at 300K. The Pd, S, O, and H atoms are shown in purple, yellow, red, and light gray, respectively. The H atoms of H_2O in the nearest neighbor of ground-state Pd_5S_7 were shown in cyan for visual clarity. The hydrogen bonds are indicated by dashed cyan lines. (**b**) Time evolution of total energy (orange) and bond angle of the H_2O molecule in the nearest neighbor of ground-state Pd_5S_7 (green). The black dashed line shows the bond angle of free H_2O molecule. (**c**) Time evolution of representative interatomic distances in the ground-state Pd_5S_7 cluster and the nearest-neighboring H_2O molecule. The free energy diagrams of CO_2 reduction and HCOOH dehydrogenation process on (**d** and **e**) ground-state Pd_5S_7 in solvation media, respectively. The inset arrows and numbers indicate the rate-determining step and the corresponding Gibbs free energy to overcome.

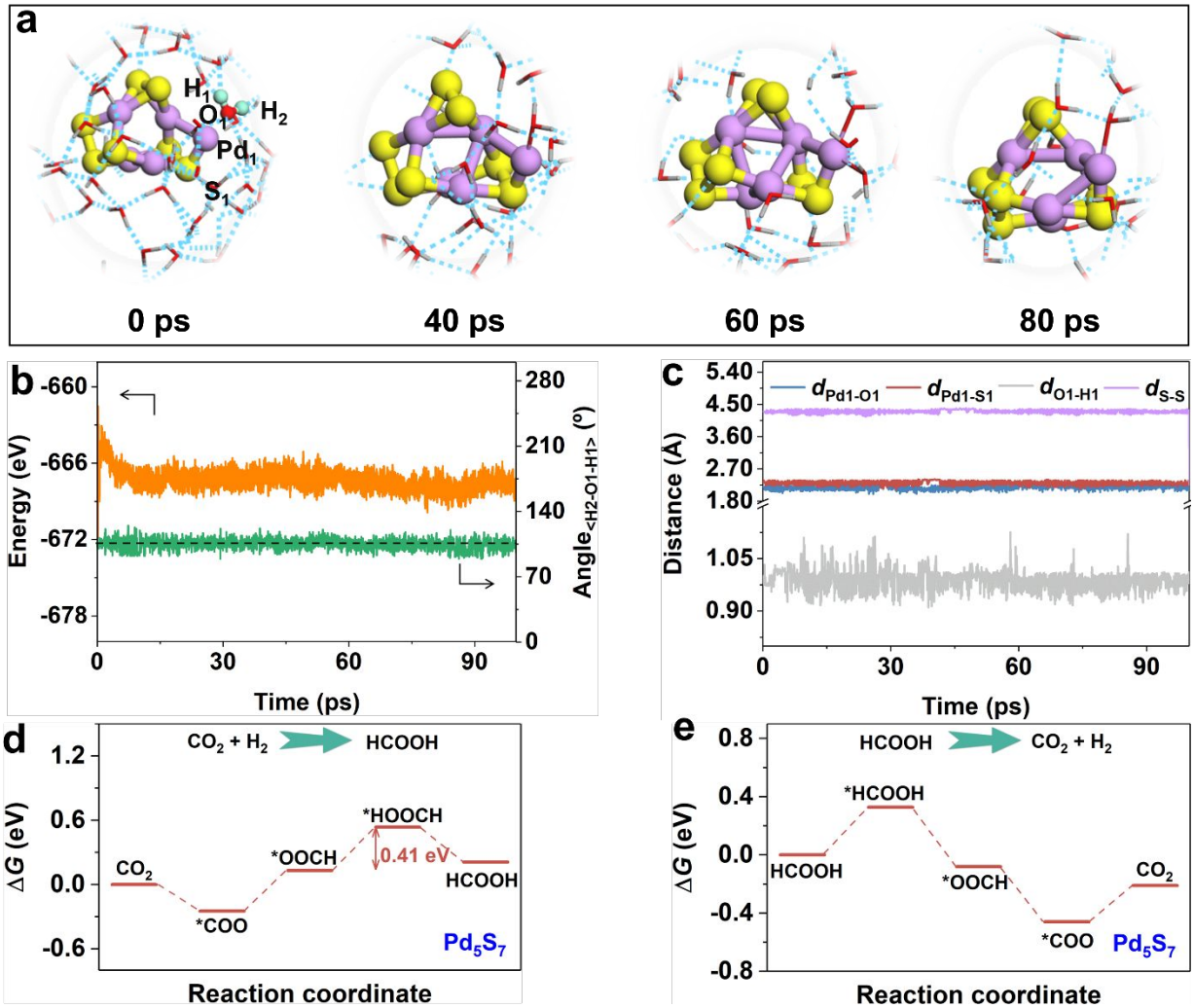

Figure S29. (**a**) Snapshots of the atomic structures of metastable Pd_5S_7 cluster in water by AIMD simulations of 0, 40, 60 and 80 ps at 300K. The Pd, S, O, and H atoms are shown in purple, yellow, red, and light gray, respectively. The H atoms of H_2O in the nearest neighbor of metastable Pd_5S_7 were shown in cyan for visual clarity. The hydrogen bonds are indicated by dashed cyan lines. (**b**) Time evolution of total energy (orange) and bond angle of the H_2O molecule in the nearest neighbor of metastable Pd_5S_7 (green). The black dashed line shows the bond angle of free H_2O molecule. (**c**) Time evolution of representative interatomic distances in the metastable Pd_5S_7 cluster and the nearest-neighboring H_2O molecule. The free energy diagrams of CO_2 reduction and HCOOH dehydrogenation process on (**d** and **e**) metastable Pd_5S_7 in solvation media, respectively. The inset arrows and numbers indicate the rate-determining step and the corresponding Gibbs free energy to overcome.

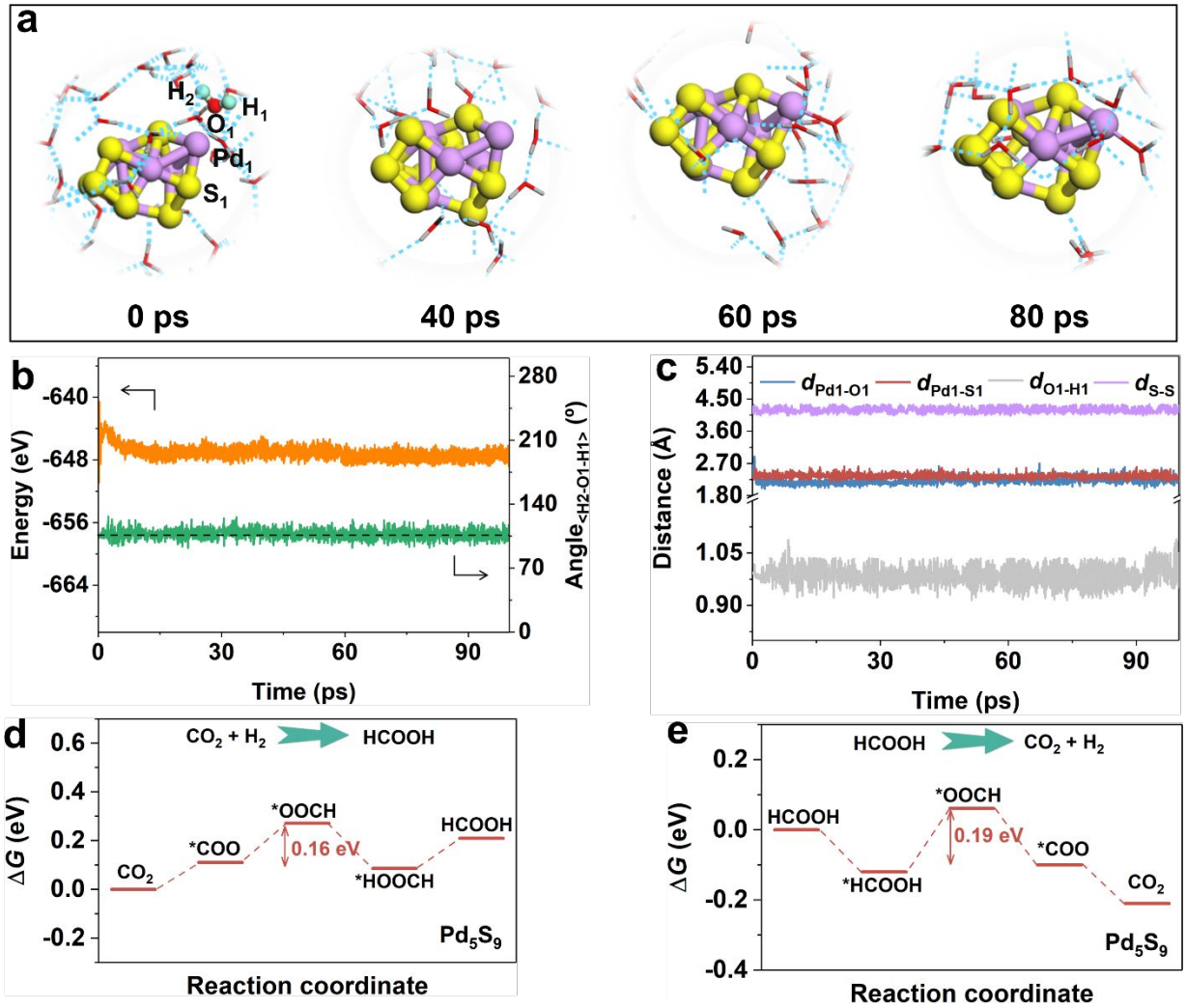

Figure S30. (**a**) Snapshots of the atomic structures of Pd_5S_9 cluster in water by AIMD simulations of 0, 40, 60 and 80 ps at 300K. The Pd, S, O, and H atoms are shown in purple, yellow, red, and light gray, respectively. The H atoms of H_2O in the nearest neighbor of Pd_5S_9 were shown in cyan for visual clarity. The hydrogen bonds are indicated by dashed cyan lines. (**b**) Time evolution of total energy (orange) and bond angle of the H_2O molecule in the nearest neighbor of Pd_5S_9 (green). The black dashed line shows the bond angle of free H_2O molecule. (**c**) Time evolution of representative interatomic distances in the Pd_5S_9 cluster and the nearest-neighboring H_2O molecule. The free energy diagrams of CO_2 reduction and HCOOH dehydrogenation process on (**d** and **e**) Pd_5S_9 in solvation media, respectively. The inset arrows and numbers indicate the rate-determining step and the corresponding Gibbs free energy to overcome.

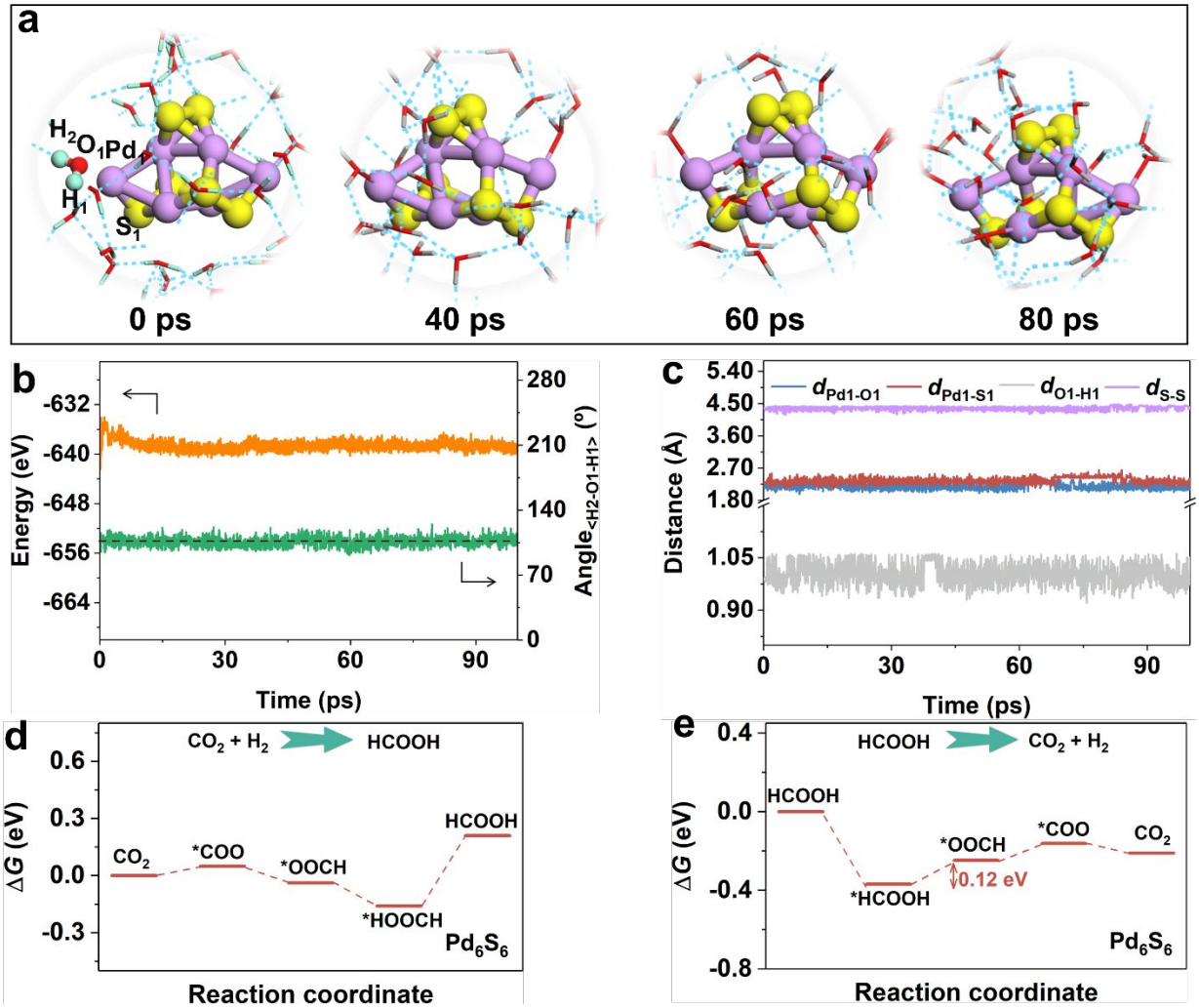

Figure S31. (**a**) Snapshots of the atomic structures of Pd_6S_6 cluster in water by AIMD simulations of 0, 40, 60 and 80 ps at 300K. The Pd, S, O, and H atoms are shown in purple, yellow, red, and light gray, respectively. The H atoms of H_2O in the nearest neighbor of Pd_6S_6 were shown in cyan for visual clarity. The hydrogen bonds are indicated by dashed cyan lines. (**b**) Time evolution of total energy (orange) and bond angle of the H_2O molecule in the nearest neighbor of Pd_6S_6 (green). The black dashed line shows the bond angle of free H_2O molecule. (**c**) Time evolution of representative interatomic distances in the Pd_6S_6 cluster and the nearest-neighboring H_2O molecule. The free energy diagrams of CO_2 reduction and HCOOH dehydrogenation process on (**d** and **e**) Pd_6S_6 in solvation media, respectively. The inset arrows and numbers indicate the rate-determining step and the corresponding Gibbs free energy to overcome.

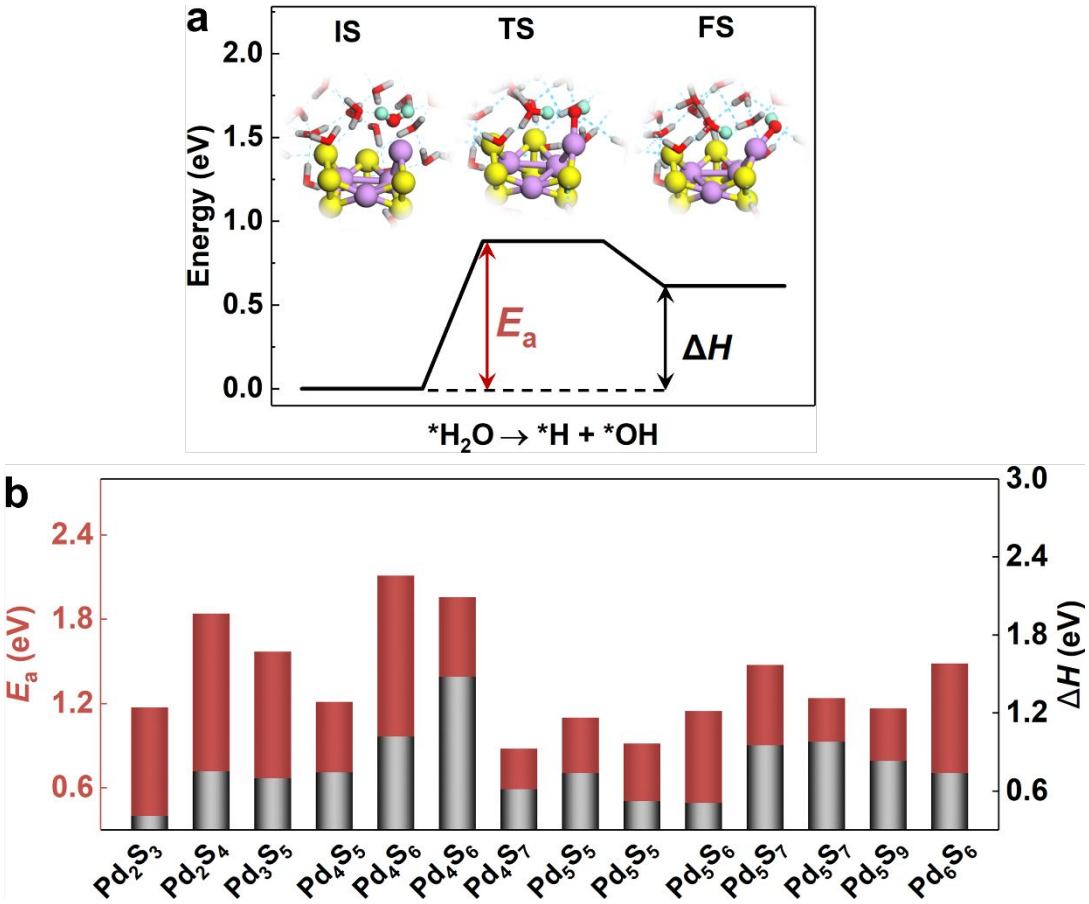

Figure S32. (a) Kinetic process of H_2O dissociation (*H_2O → *H + *OH) on Pd_4S_7 cluster in water media. The initial state (IS), the transition state (TS) and the final state (FS) are indicated in the diagram. (b) Kinetic barriers (E_a) and reaction heat (ΔH) of water dissociation on 14 Pd_xS_y clusters.

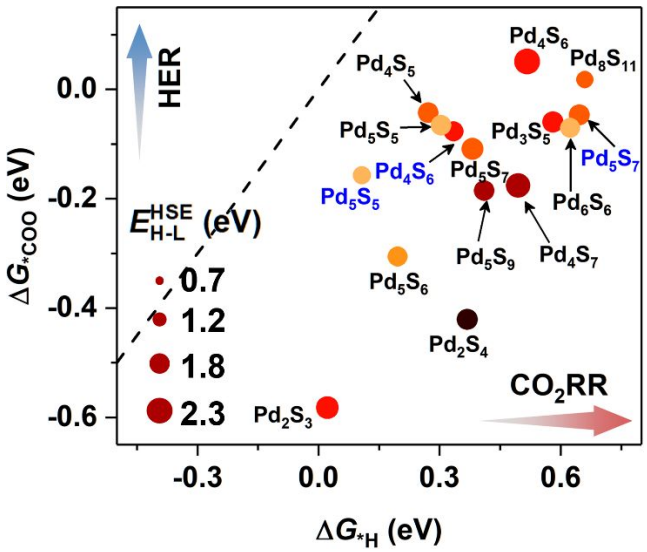

Figure S33. Comparison of adsorption free energies between CO_2 molecule (ΔG_{*COO}) and *H species (ΔG_{*H}) on Pd_xS_y clusters. The symbol size is proportional to *E*HSE H-L of Pd_xS_y clusters.

Supporting references

(1) Zhao, J.; Shi, R.; Sai, L.; Huang, X.; Su, Y., Comprehensive Genetic Algorithm for *Ab Initio* Global Optimisation of Clusters. *Mol. Simulat.* **2016,** *42*, 809–819.

(2) Delley, B., From Molecules to Solids with the DMol^3 Approach. *J. Chem. Phys.* **2000,** *113*, 7756–7764.

(3) Perdew, J. P.; Burke, K.; Ernzerhof, M., Generalized Gradient Approximation Made Simple. *Phys. Rev. Lett.* **1996,** *77*, 3865.

(4) Heyd, J.; Scuseria, G. E.; Ernzerhof, M., Hybrid Functionals Based on a Screened Coulomb Potential. *J. Chem. Phys.* **2003,** *118*, 8207–8215.

(5) Chase, M. W., NIST-JANAF Thermochemical Tables for Oxygen Fluorides. *J. Phys. Chem. Ref. Data* **1996,** *25*, 551–603.